Edwin Mierkiewicz
The Earth's Hydrogen Corona

University of Wisconsin
(emierk@astro.wisc.edu)

| Thank You:	NSF	CSSC
Fred Roesler	Robert Meier	Wenbin Wang
Susan Nossal	Geoff Crowley	Alan Burns
James Bishop	Sam Yee	Bob Kerr
Matt Haffner	Andy Stephan	John Noto
Ron Reynolds	Elsayeed Taalat	Lara Waldrop

The idea of a diffuse hydrogen corona surrounding the earth (i.e.,the geocorona) -- and its possible thermal escape -- dates back to the mid 19th century

– The first real detection would have to wait until the space age…

The modern era of geocoronal research began in 1955 with the detection of intense (hydrogen) Lyman alpha "nightglow" at altitudes above 75 km by a NRL sounding rocket

- early controversy… terrestrial, interplanetary??
- eventually revealed that the emission was due to the resonant scattering of solar Lyman alpha photons by geocoronal hydrogen

*The modern era of geocoronal research began in 1955 with the
detection of intense (hydrogen) Lyman alpha "nightglow" at
altitudes above 75 km by a NRL sounding rocket*
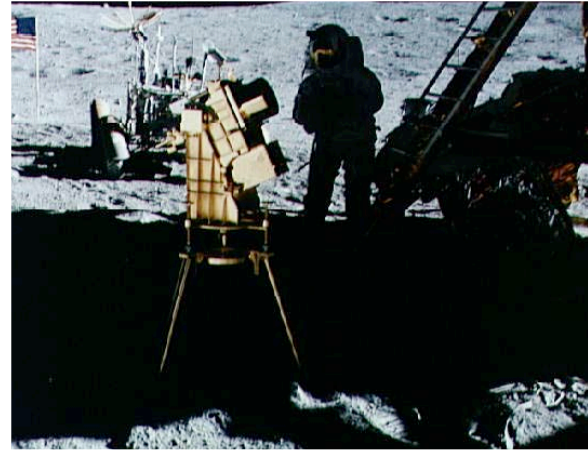
NASA Apollo 16 Archive

- – early controversy… terrestrial, interplanetary??
- – eventually revealed that the emission was due to the resonant scattering of solar Lyman alpha photons by geocoronal hydrogen

Why is this interesting?

Chemistry
Escape
Evolution
Physics
Global change

3

H escape

Atomic hydrogen
increasingly dominant
with altitude

2

CH_4, H_2O, H_2 chemistry
& photolysis reactions

1

Sources of methane:
wetlands, farming/livestock,
biomass burning, industry

$\Phi(CH_4)$, $\Phi(H_2O)$, $\Phi(H_2)$

[1](http://earthobservatory.nasa.gov/Features/BiomassBurning/)
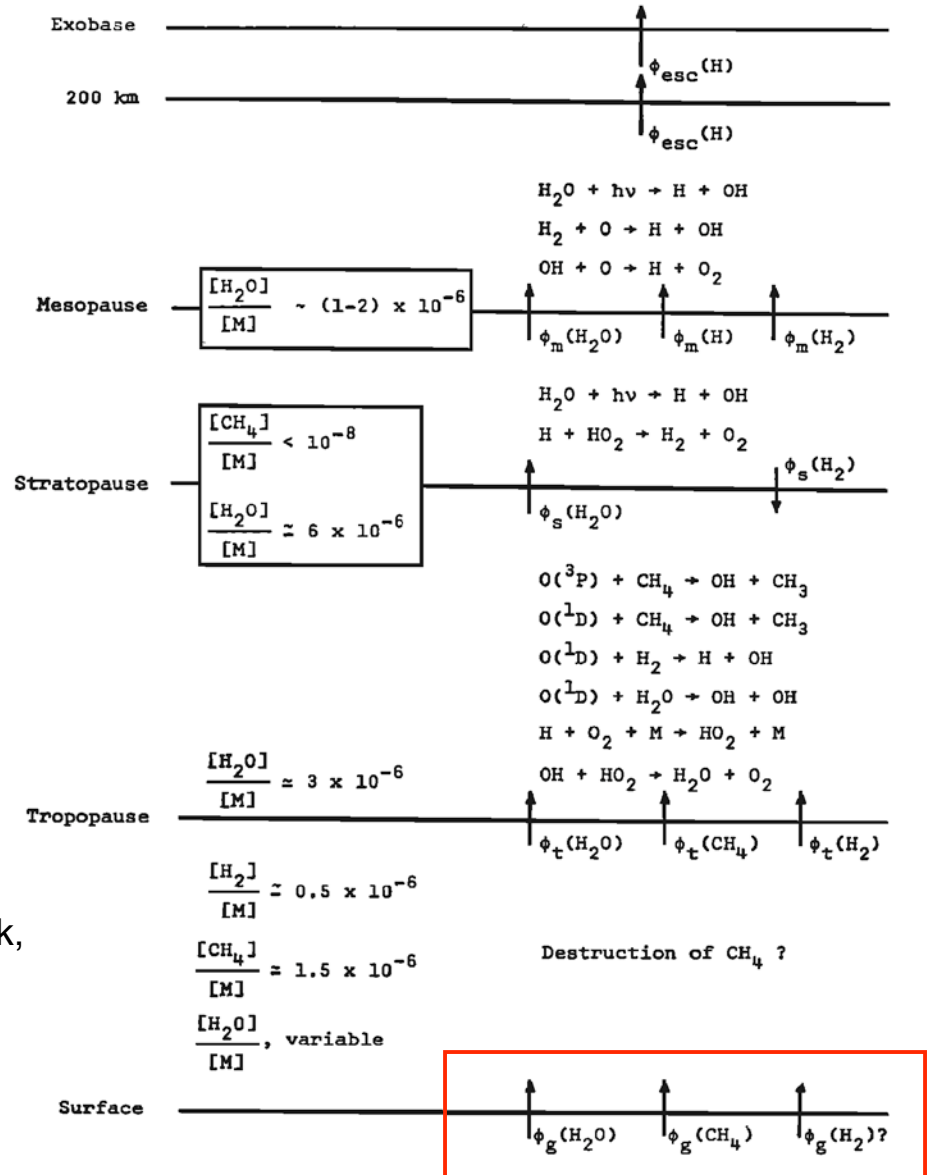
[2]© Pekka Parviainen (http://lasp.colorado.edu/noctilucent_clouds/)

[3]Carruthers et. al, 1976
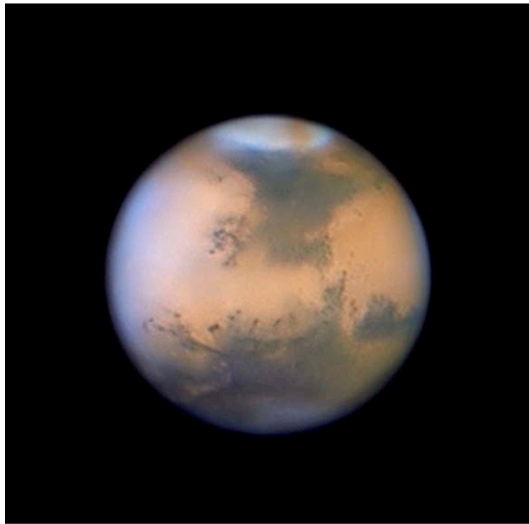
Strobel, 1972

TABLE 2. Photochemistry and transport of hydrogen constituents

(The subscripts of φ denote its magnitude at a given level.)

Evolution

exospheric physics

Jean-Luc Dauvergne, Francois Colas,
IMCCE/S2P, Obs. Midi-Pyrénées

Apollo 17 Crew, NASA

Galileo Project, JPL, NASA

HOW WILL CHANGES IN CARBON DIOXIDE AND METHANE MODIFY THE MEAN STRUCTURE OF THE MESOSPHERE AND THERMOSPHERE ?

R. G. Roble

High Altitude Observatory, National Center for Atmospheric Research

R. E. Dickinson

Climate and Global Dynamics Division, National C

Abstract. A global average model of the coupled mesosphere, thermosphere and ionosphere is used to examine the effect of trace gas variations on the overall structure of these regions. In particular, the variations caused by CO_2 and CH_4 doublings and halvings from present day mixing ratios are presented. The results indicate that the mesosphere and thermosphere temperatures will cool by about 10K and 50K respectively as the CO_2 and CH_4 mixing ratios are doubled. These regions are heated by similar amounts when the trace gas mixing ratios are halved. Compositional redistributions also occur in association with changes in the temperature profile. The results show that global change will occur in the upper atmosphere and ionosphere as well as in the lower atmosphere during the 21st century.

mimics s
trations
low trop
CO_2 and
For the o
through
tempera
cant alte
minor sp
When th
in tempe
with gen
the case
sults ind
tions is

Percent change: H (cm3)

Roble, 2010
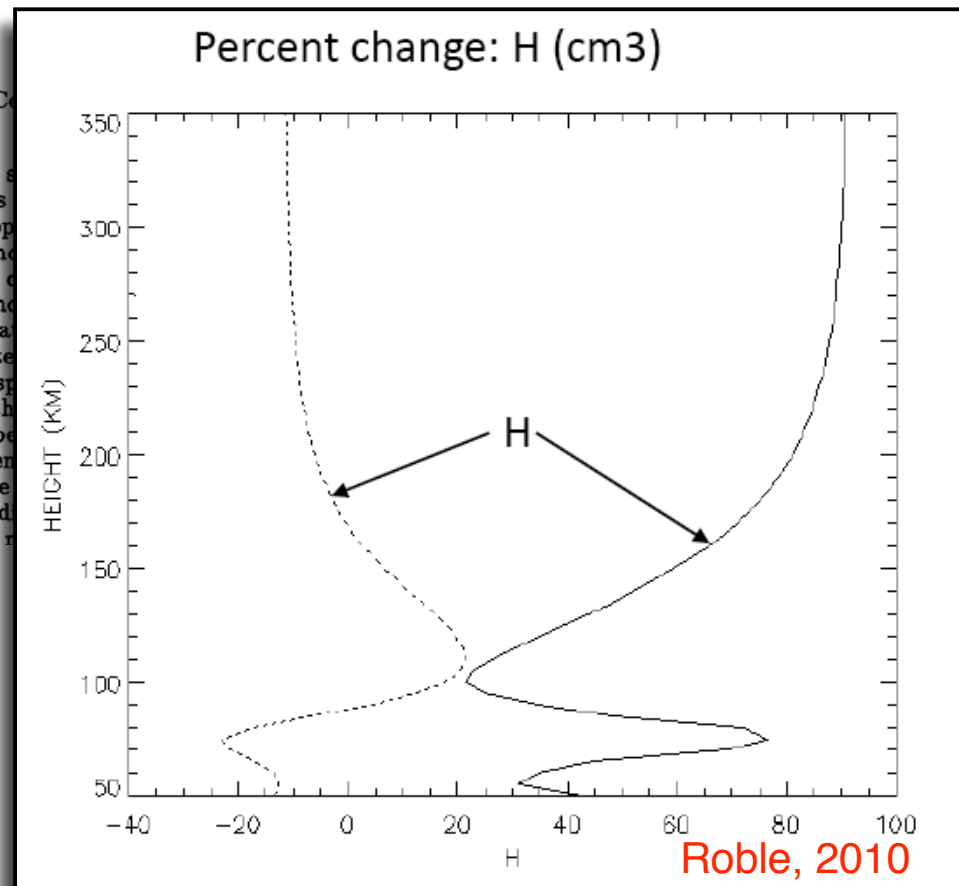
- A daughter of H_2O and CH_4
  - distribution in the mesosphere and lower thermosphere is a key parameter in understanding the chemistry of the upper atmosphere (MLT photochemistry and dynamics)

- Planetary escape and the distribution of atomic hydrogen out into the interplanetary medium
  - role in planetary evolution and exospheric phenomena

- Inconsistent observational evidence for H's mean state in the thermosphere and exosphere (e.g., seasonal variability and response to solar forcing)
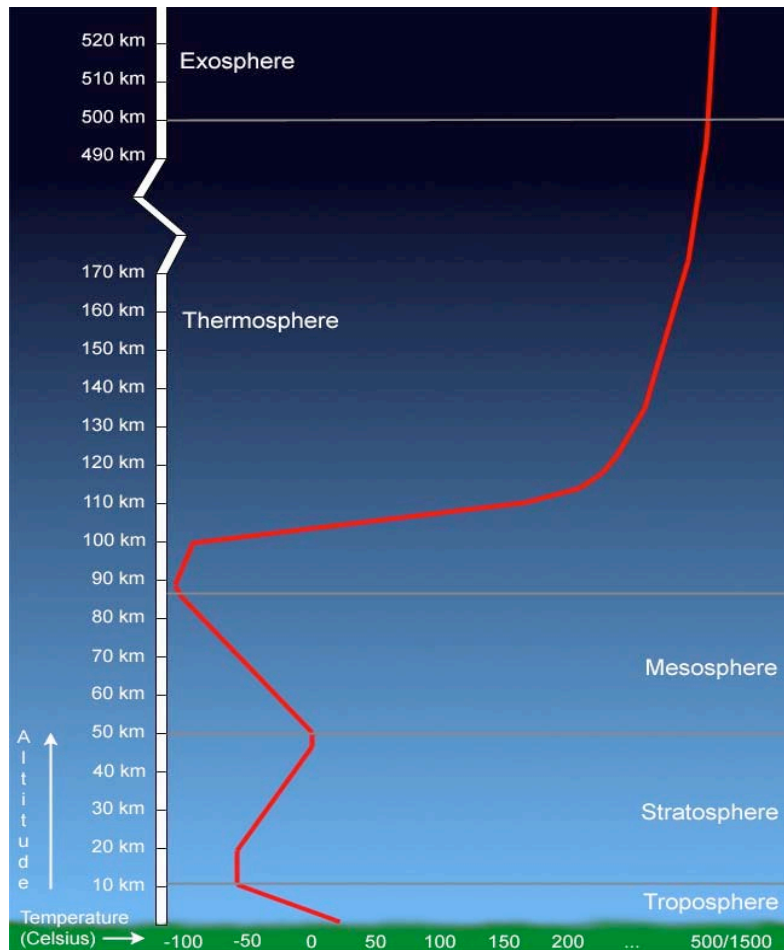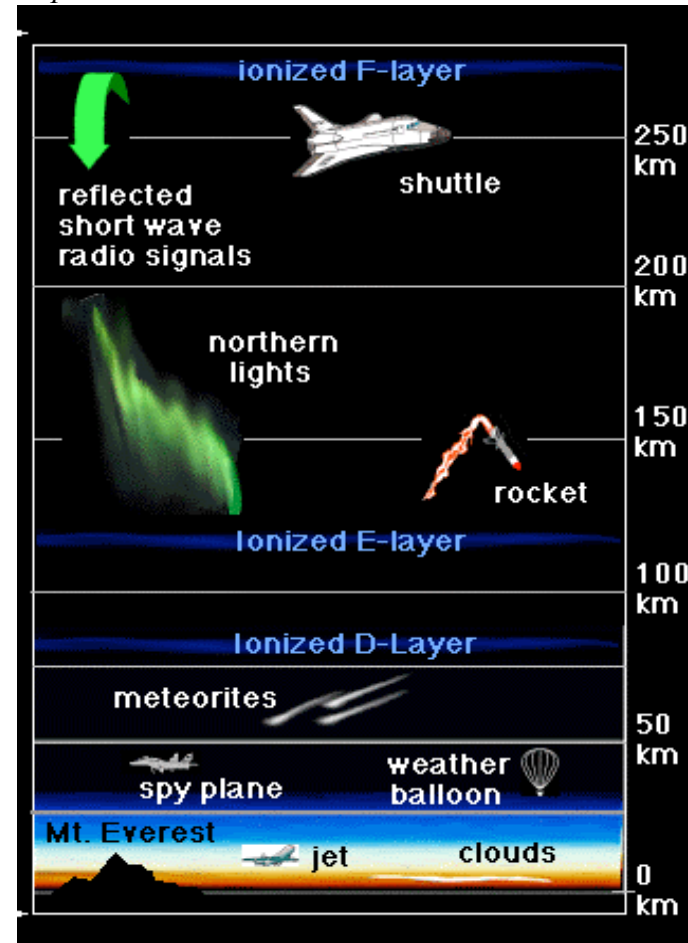
Okay, now take a step back…

Regions
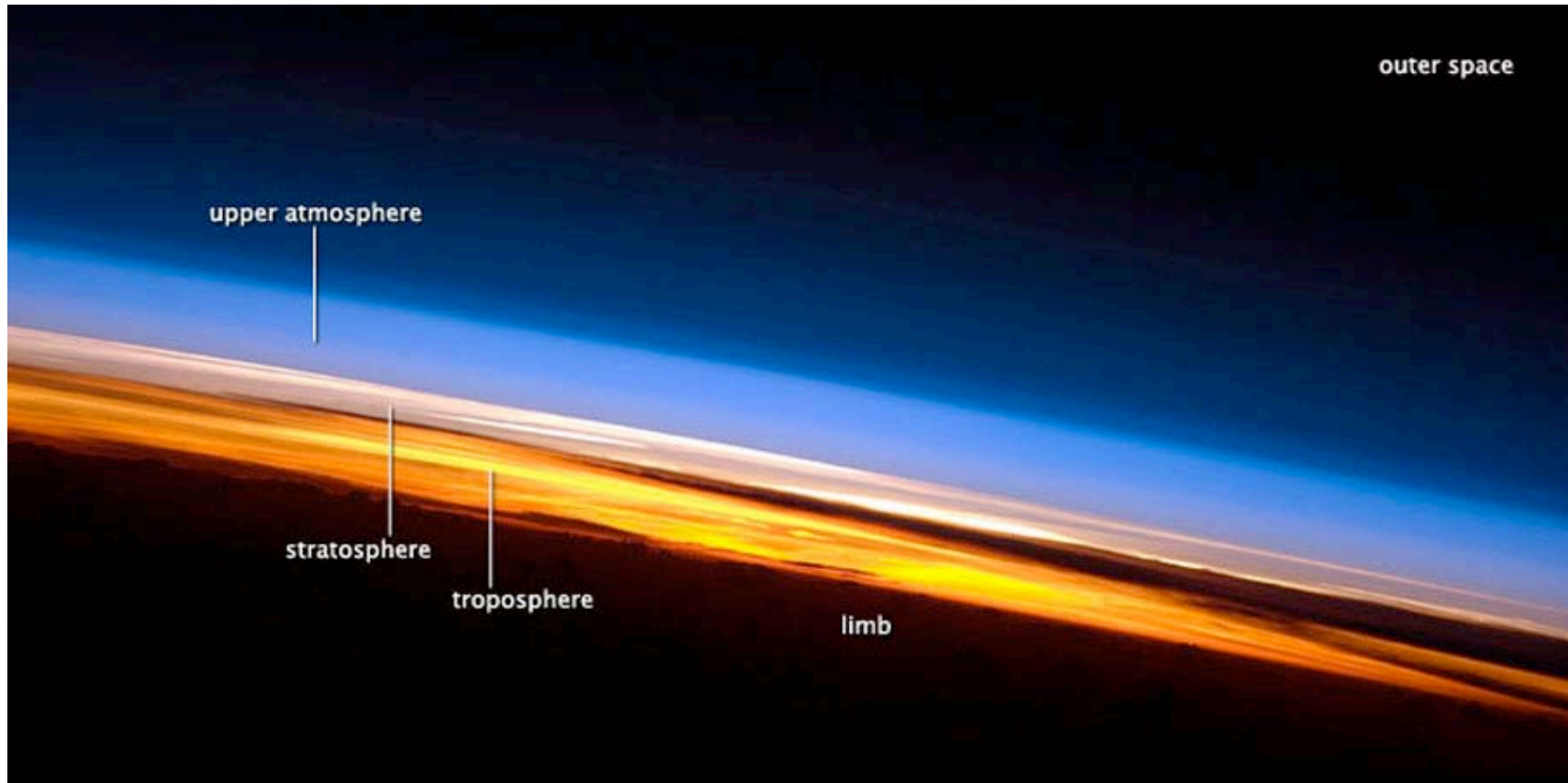
Expedition 23 Crew, NASA

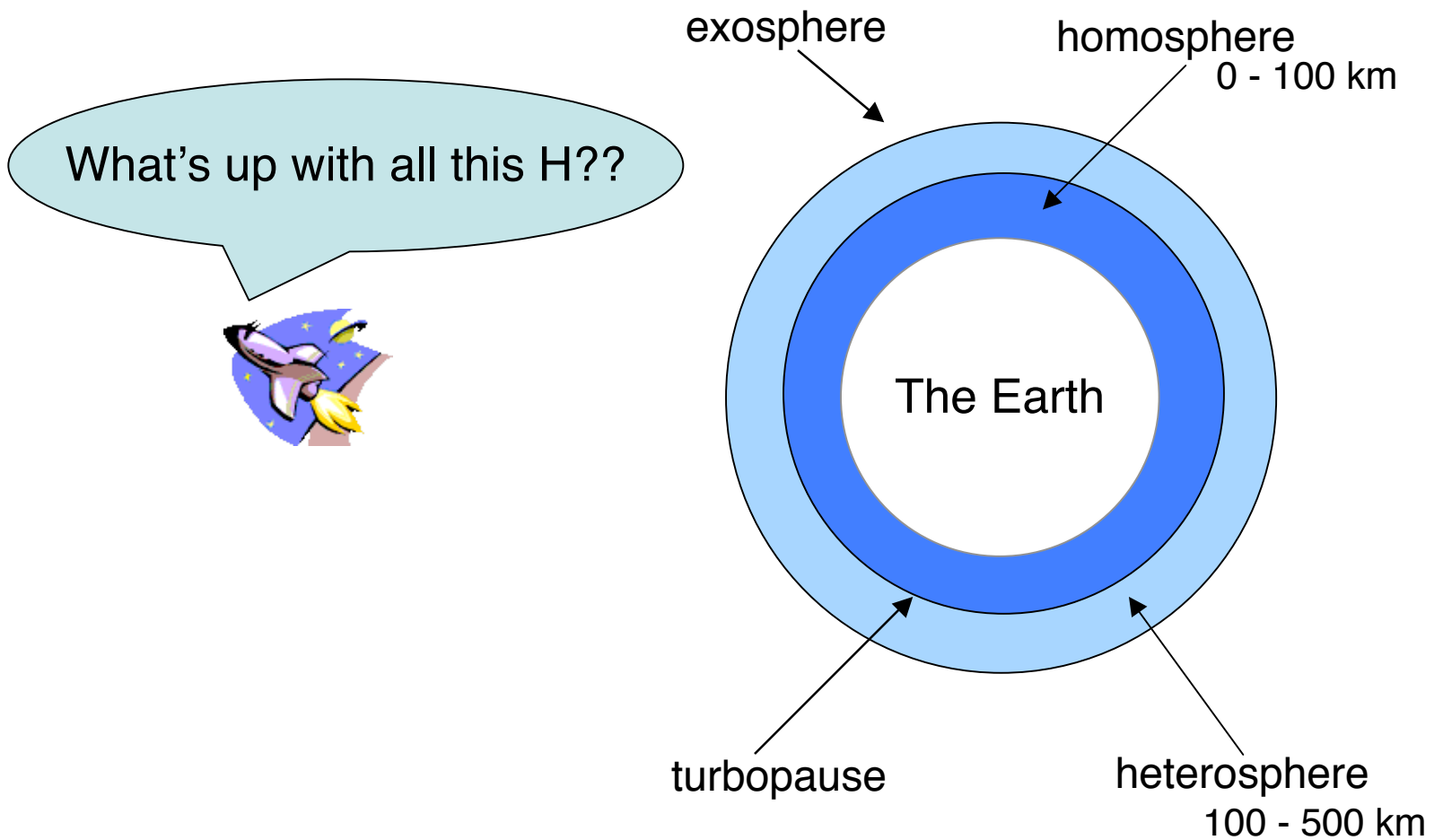# Regions

defined by gradients in temperature

http://www.windows.ucar.edu/

-- ionization & other stuff --

Regions

defined by gradients in composition

Flow

$$\Phi_i = -D_i n_i \left(\frac{1}{n_i} \frac{dn_i}{dz} + \frac{m_i g}{kT} + \frac{(1 + \alpha_T^i)}{T} \frac{dT}{dz} \right) - K n_i \left(\frac{1}{n_i} \frac{dn_i}{dz} + \frac{m_a g}{kT} + \frac{1}{T} \frac{dT}{dz} \right)$$

above 100 km   below 100 km

- Turbulent mixing and molecular diffusion are competing processes in the atmosphere
  - leads to changes in atmospheric mixing & composition with altitude
- Eddy diffusion dominates below 100 km ($K >> D_i$)
  - turbulent well mixed atmosphere
  - homosphere
- Molecular diffusion dominates above 100 km ($K << D_i$)
  - tends to produce an atmosphere with species-wise density profiles
  - heterosphere

Hydrostatic

$$\Phi_i = -D_i n_i \left(\underbrace{\frac{1}{n_i}\frac{dn_i}{dz} + \boxed{\frac{m_i g}{kT}}}_{\text{above 100 km}}^{1/H_i} + \frac{(1+\alpha_T^i)}{T}\frac{dT}{dz} \right) - K n_i \left(\underbrace{\frac{1}{n_i}\frac{dn_i}{dz} + \boxed{\frac{m_a g}{kT}}}_{\text{below 100 km}}^{1/H} + \frac{1}{T}\frac{dT}{dz} \right)$$

- Make some assumptions… isothermal, $\Phi = 0$…
  - hydrostatic equilibrium

$$n = n_o \exp(-z/H)$$
$$n_i = n_{io} \exp(-z/H_i)$$

- The quantity H is known as the scale height
  - *H* is an important parameter in any atmosphere
  - *e*-folding distance
  - essentially the rate at which pressure (density) changes with altitude
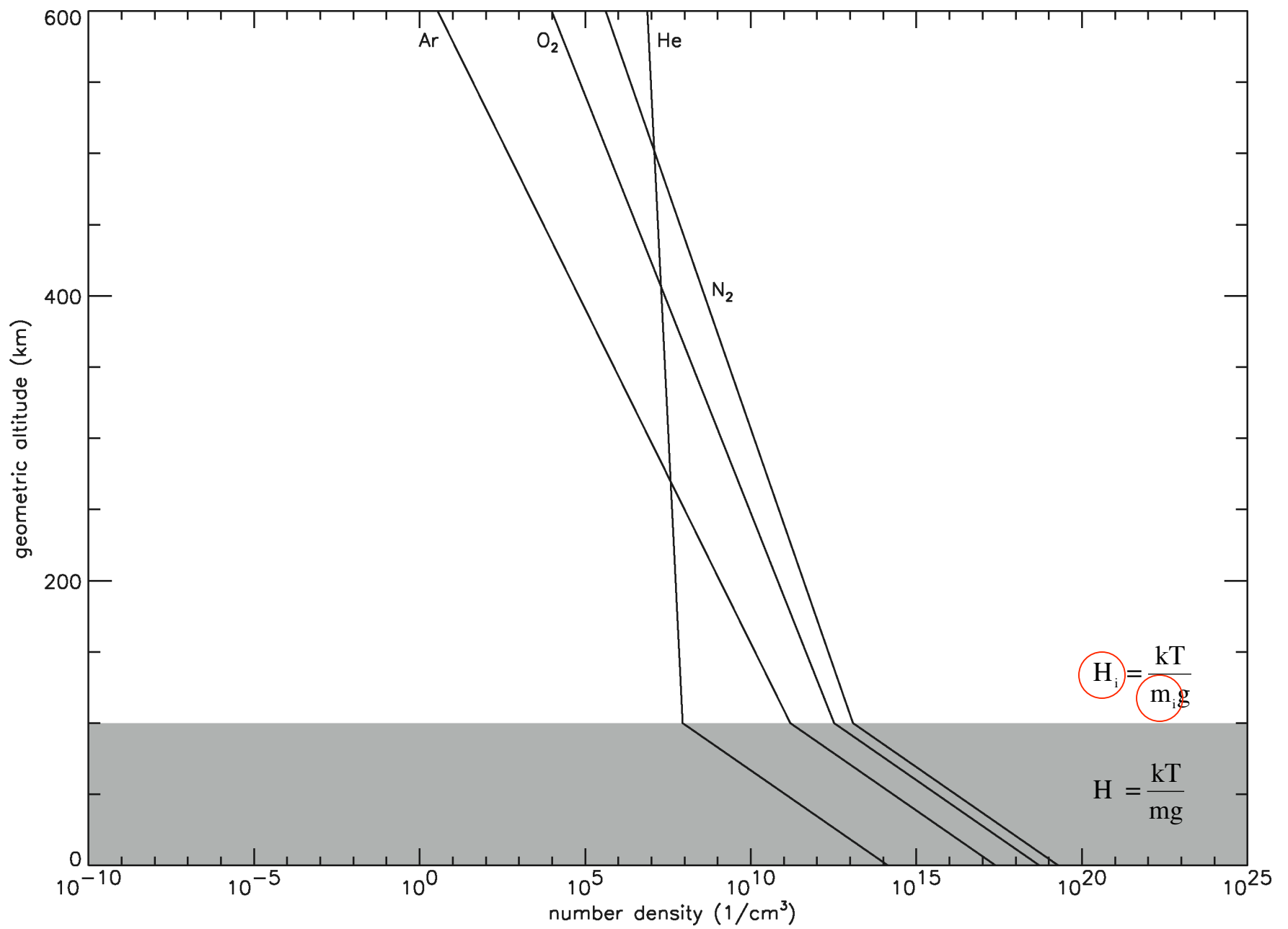 - the smaller the scale height, the faster the decrease
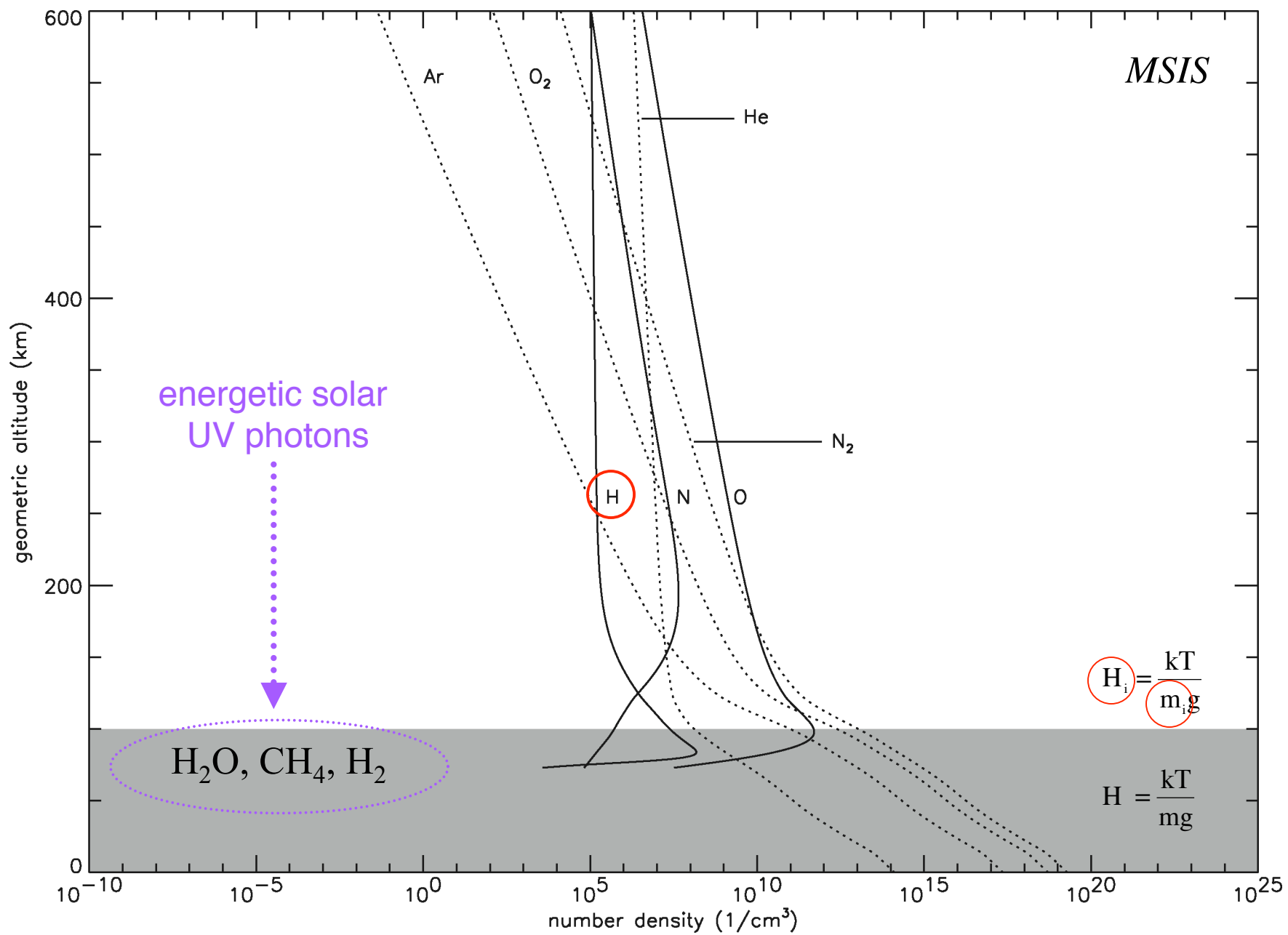
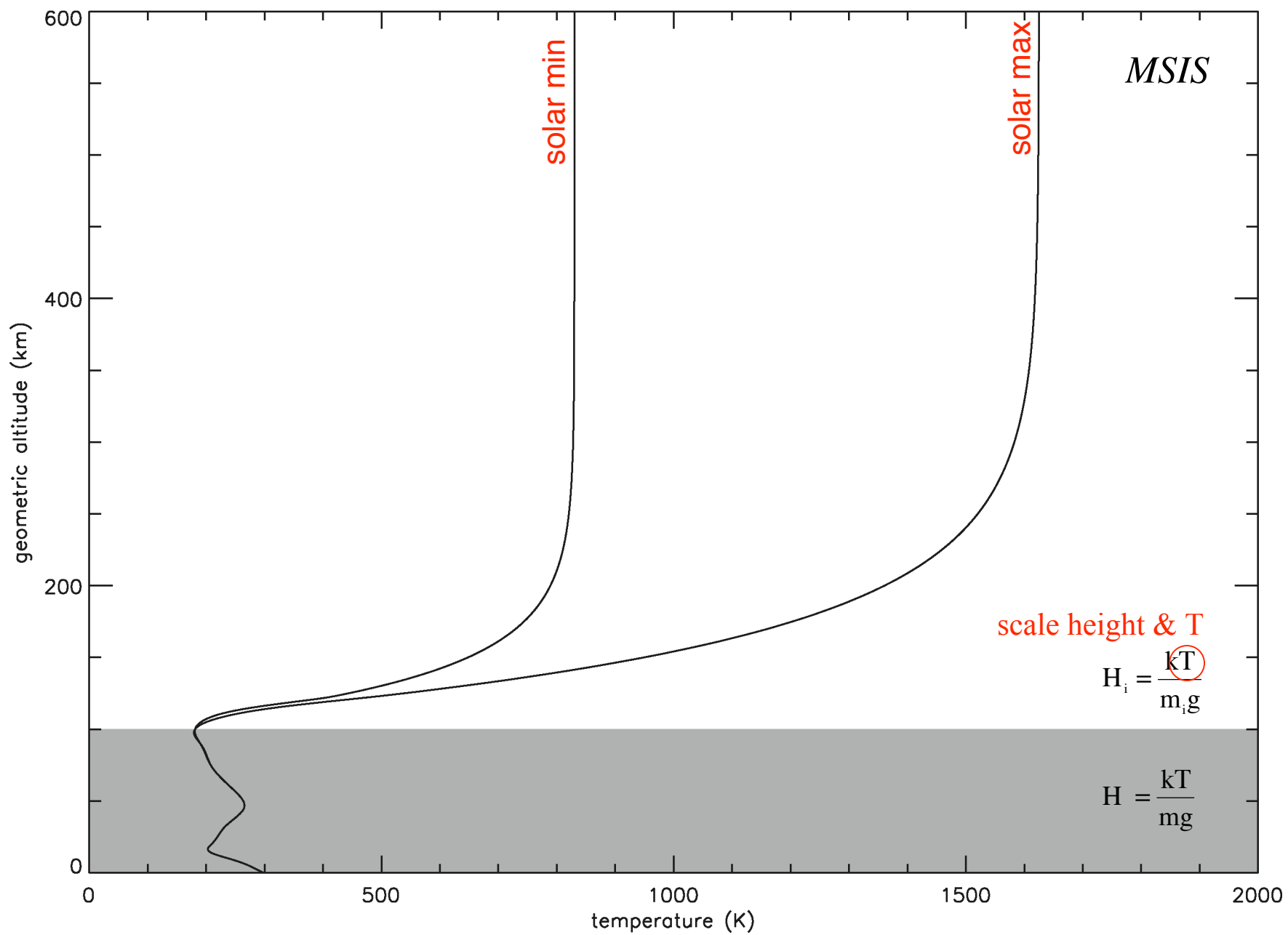# A simple two layer hydrostatic model

Model assumptions below 100 km:

- Well mixed with a mean molecular mass M = 28.97 (dry air)

- Isothermal with T = 250 K

- g(z) = const. = 9.8 m/s^2

- Results in a constant scale height: H = 7 km

- U.S. standard atmosphere number density:

  n_{sfc} = 2.5 x 10^{19} cm^{-3}

Model assumptions above 100 km:

- Molecular diffusion dominates

- Isothermal with T = 960 K

- Each constituent with its own scale height (based on mass)

- Number densities matched at 100 km

The Earth's Hydrogen Corona — Mierkiewicz, CEDAR 2010

The Earth's Hydrogen Corona — Mierkiewicz, CEDAR 2010

The Earth's Hydrogen Corona — Mierkiewicz, CEDAR 2010

or the tenuous uppermost reach of the earth's neutral atmosphere

The Exosphere

Is a Death Metal Band From Holland

Exobase

- In the barosphere (homosphere & heterosphere) atoms & molecules interact through frequent collisions
  - thermal (Maxwellian) kinetic distributions

- **As mean free path is inversely proportional to number density, a level is eventually reached where mfp > H**
  - density $\downarrow$ mfp $\uparrow$ ($\text{mfp}_{sfc}=10^{-7}$ m)
  - collisions are less and less likely…
  - the atmosphere can no longer be treated as a fluid

- The exobase is defined as the level at which mfp = H
  - classical treatment of the exosphere assumes a Maxwell-Boltzman distribution below r_c and a collisionless region above r_c

PLANETARY CORONAE AND ATMOSPHERIC EVAPORATION*

JOSEPH W. CHAMBERLAIN

Kitt Peak National Observatory,† Tucson, Arizona

Abstract—A comprehensive theory is presented for the region of a planetary atmosphere where collisions are rare and where the controlling factors are gravitational attraction and thermal energy conducted from below. Although the subject of this article originated literally with the kinetic theory itself, until recently attention has been confined to atmospheric evaporation.

- Classical treatment assumes a Maxwellian distribution below r_c (exobase) and a collisionless region above

- Velocity distribution is determined by the free motion of particles in a gravitational field

  - divided into 3 populations based on whether or not their kinetic energy exceeds the earth's gravitational potential and whether or not their trajectory intersects the exobase

    Ballistic, Satellite, & Escape

Velocity distribution

satellite critical level r_{sc}

exosphere

The Earth

heterosphere

the exobase (~500 km)
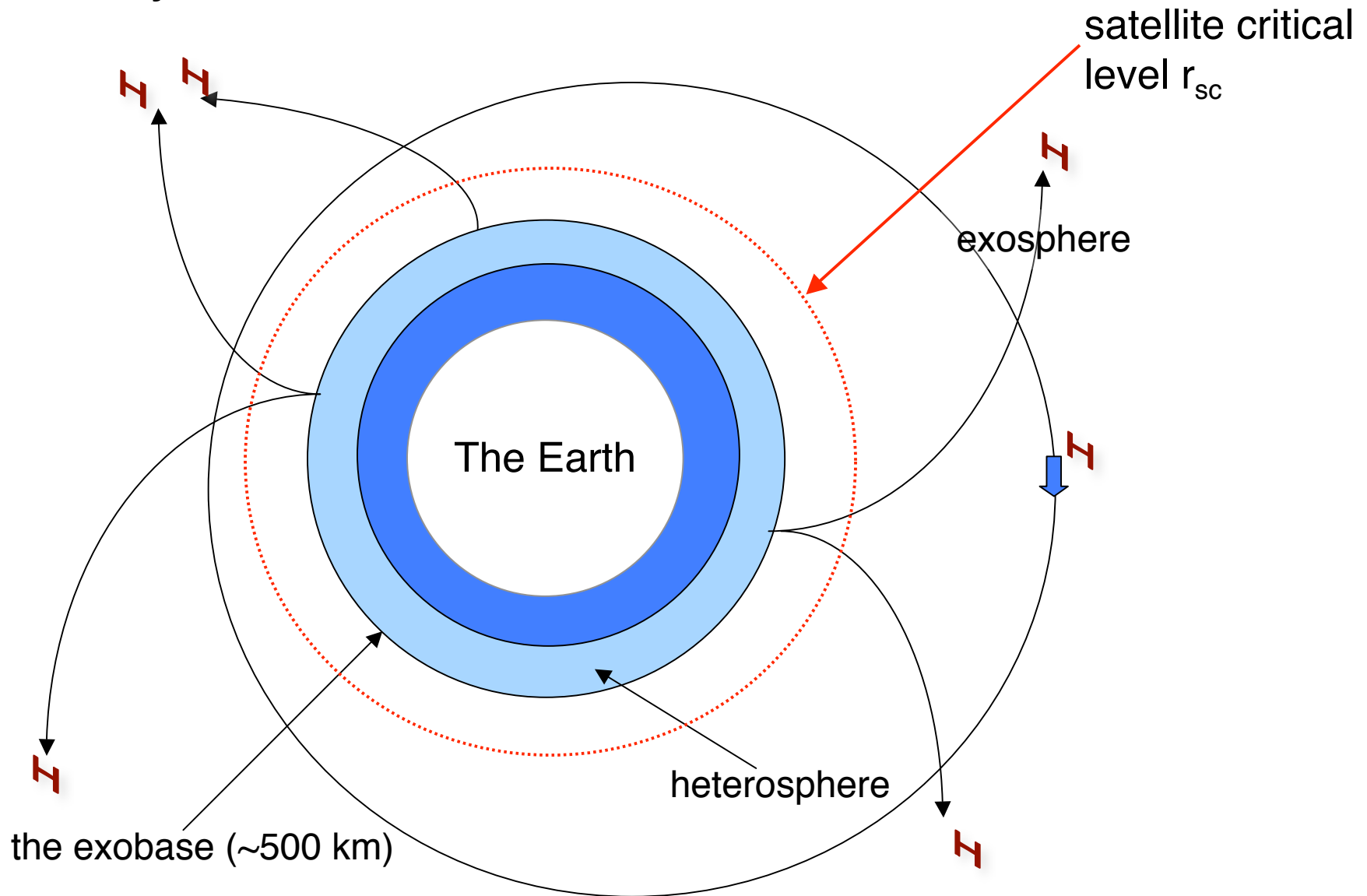
Escape

- Neglecting collisions, a particle moving vertically upward will escape from the earth's gravitational field if its KE > PE:

$$\frac{1}{2}mv^2 > mg(r)r$$

  - solving, v_e=10.77 km/s at 500 km

- For a gas in TE the most probable molecular velocity is:

$$u = \sqrt{\frac{2kT}{m}}$$

  - If $u > v_e$ the gas will flow out like a fluid (e.g., the solar wind)
  - for present day exospheric temperatures this rapid escape cannot occur

Salby, Atmospheric physics
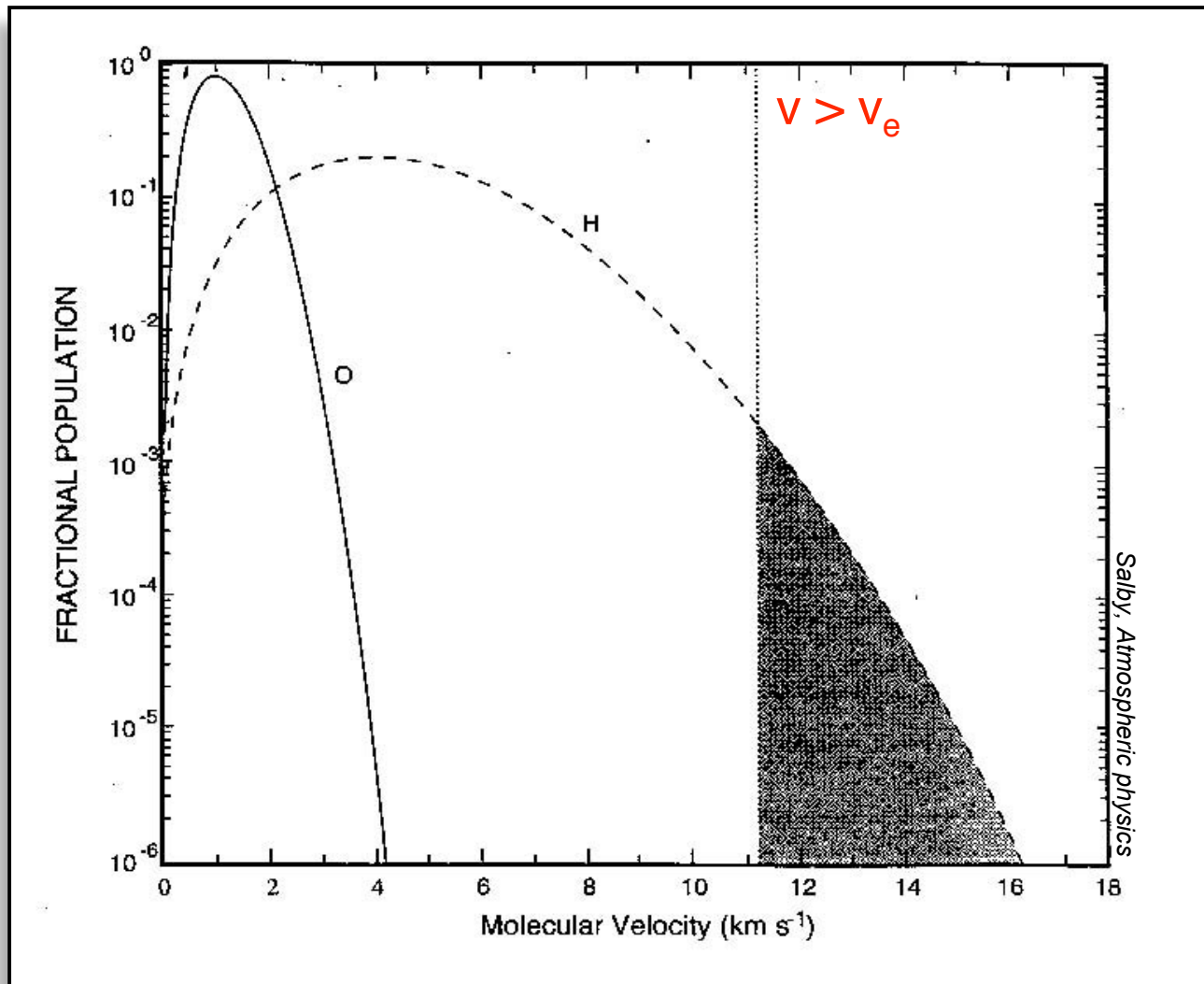
- The maximum thermal production of escaping atoms will occur near the exobase where the density is high enough to maintain a significant collision rate, yet small enough (in the vertical) to permit high velocity atoms to actually escape
  - thermal (Jeans) escape flux for H: $\sim 7 \times 10^7$ atoms cm^{-2} s^{-1}

- In order to escape, hydrogen must first get to the exosphere
  - flow through the lower atmosphere sets this limit

- Limiting flux concept…
  - estimates of the upward flow of H from the lower atmosphere implies an escape flux of:
    $\sim 3 \times 10^8$ atoms cm^{-2} s^{-1}
  - assumed constant over a solar cycle
  - this escape flux over geological time scales may be sufficient to generate the present day O content of the atmosphere
  - thermal (Jeans) escape flux is a factor of ~ 2-3 times too low

There's more than one way to escape!

charge exchange, polar wind

Tinsley, 1973 (Cole, 1966)

$$H + H^+_{hot} \rightarrow H_{hot} + H^+$$
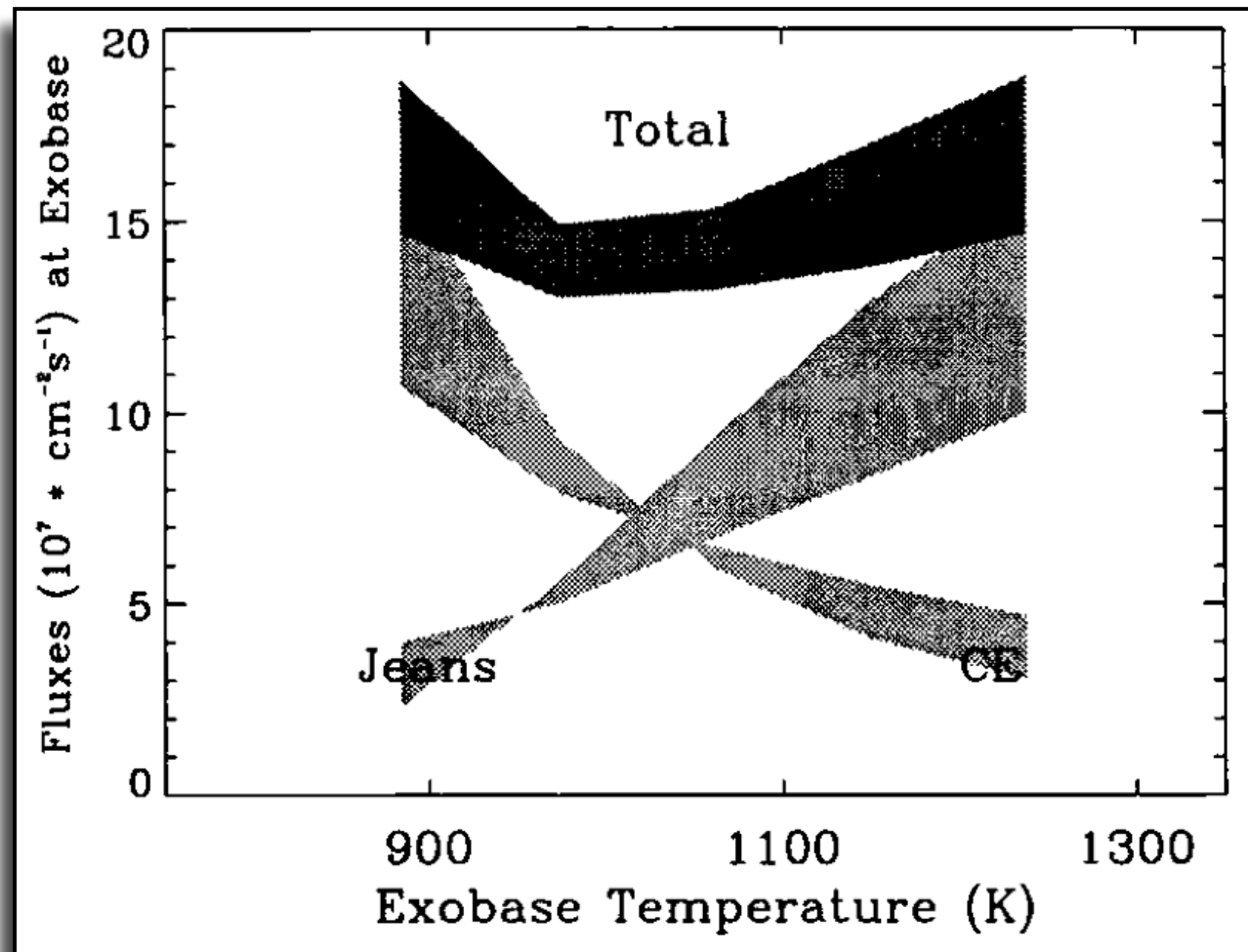
$$H^+ + O \leftarrow H + O^+$$
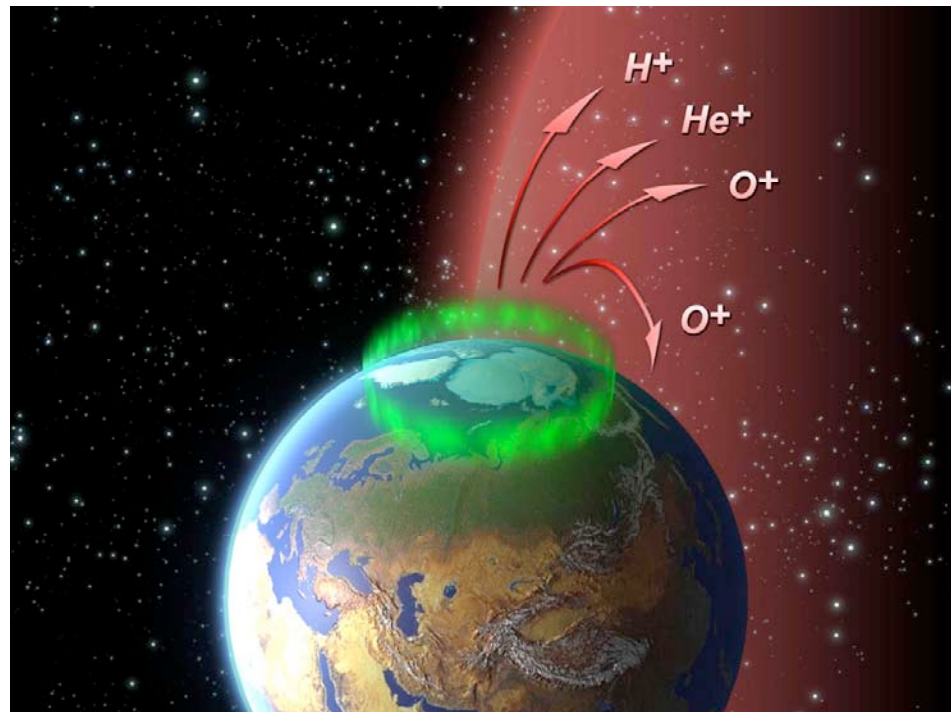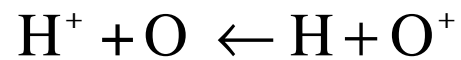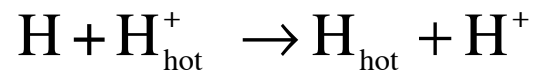
NASA/ESA

There's more than one way to escape!

total: Jeans + CE

He, BU Thesis (with Kerr), 1995

Okay, back to 1955

FAR ULTRAVIOLET RADIATION IN THE NIGHT SKY*

J. E. KUPPERIAN, Jr., E. T. BYRAM, T. A. CHUBB and H. FRIEDMAN

U.S. Naval Research Laboratory, Washington 25, D.C.

Abstract—Rocket measurements have shown that the night sky is aglow with a diffuse Lyman-α (1216 Å) emission amounting to 10^{-2} erg cm^{-2}sec^{-1} from the entire hemisphere. The glow was so bright that celestial sources of Lyman-α could not be detected through it. At wavelengths near 1300 Å discrete celestial sources were observ... from the entire sky in the wavelength interval 1225–...
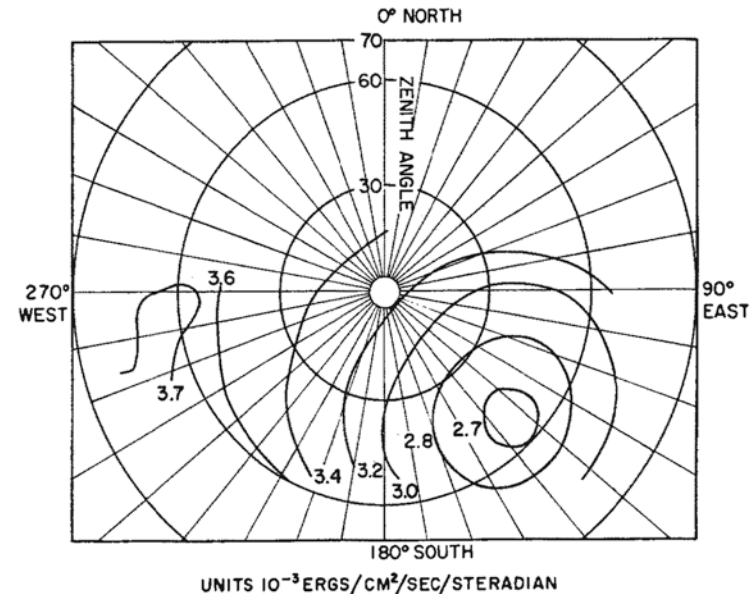

Fig. 1. Lyman-α directional intensity contours when the detector looked at the upper hemisphere. These data were obtained from the portion of the flight above 130 km and are uncorrected for the 1225 to 1350 Å discrete sources. The smallest intensity contour circle contains the anti-solar direction.

Methods

- AE Satellite Mass Spectrometers
  - H derived from in-situ composition measurements of H^+, O^+ & O
  - charge exchange equilibrium -- valid below 400 km
  - basis of MSIS H
  - e.g., Brinton et al., 1975

- Lyman-alpha (121.6 nm) & Lyman-beta (102.6 nm)
  - type of information obtained depends on the orbit
  - e.g., Meier and Mange, 1970 OSO4/OGO4
    - n_c & T_c
    - Diurnal variation of n_c ~1.8 (max ~0500 hours, min ~ 1600 hours)
  - Anderson et al., 1987 (Bush & Chakrabarti, 1995; Bishop, 1999)
    - Lyman-alpha limb scans STP 78-1, March 1979
    - [H](z)
    - gold standard

- Balmer-alpha & Balmer-beta
  - more on this later

- Abs. cells, etc…

•Diurnal variation of n_c ~1.8 (max ~0500 hours, min ~ 1600 hours)
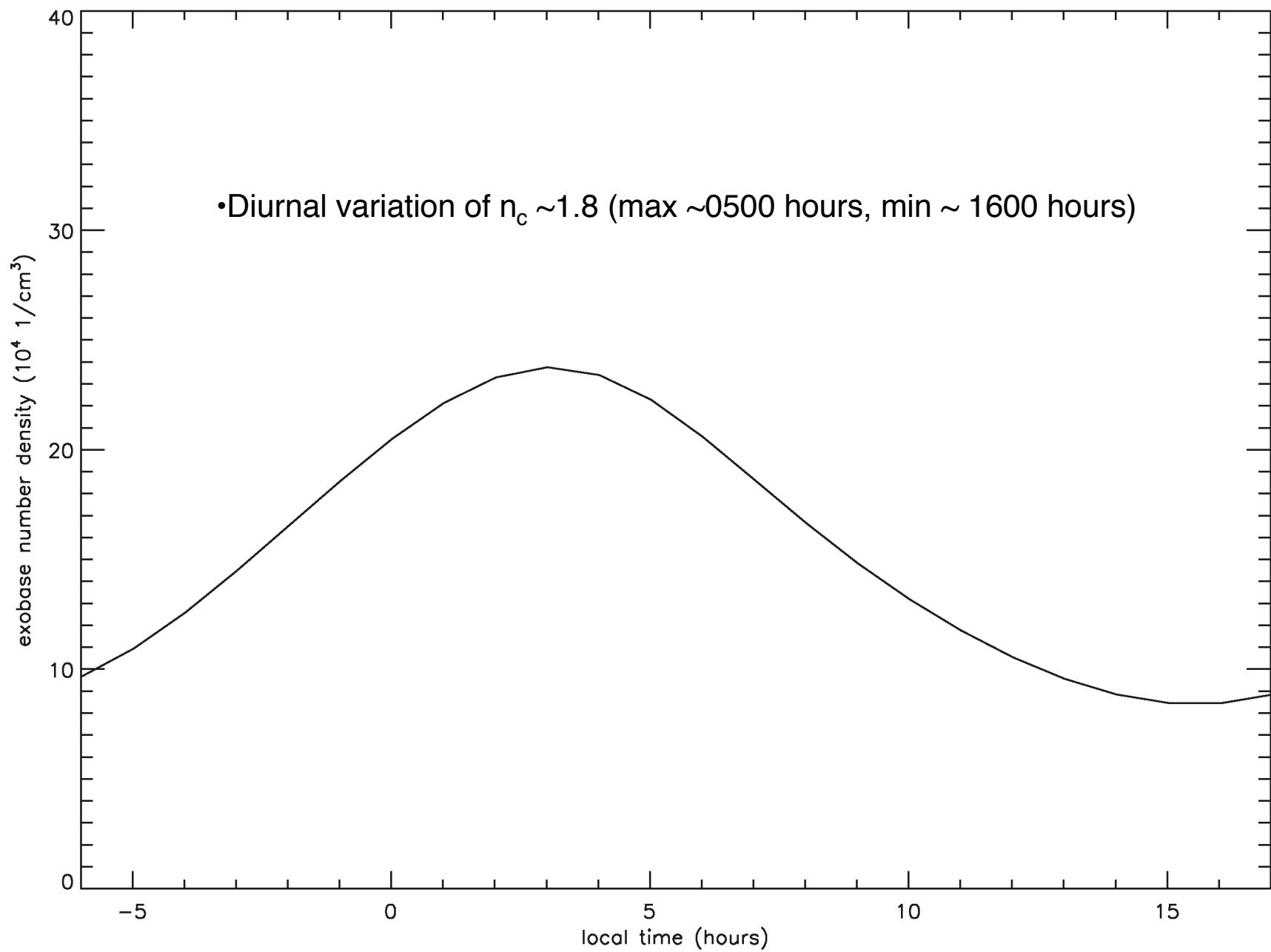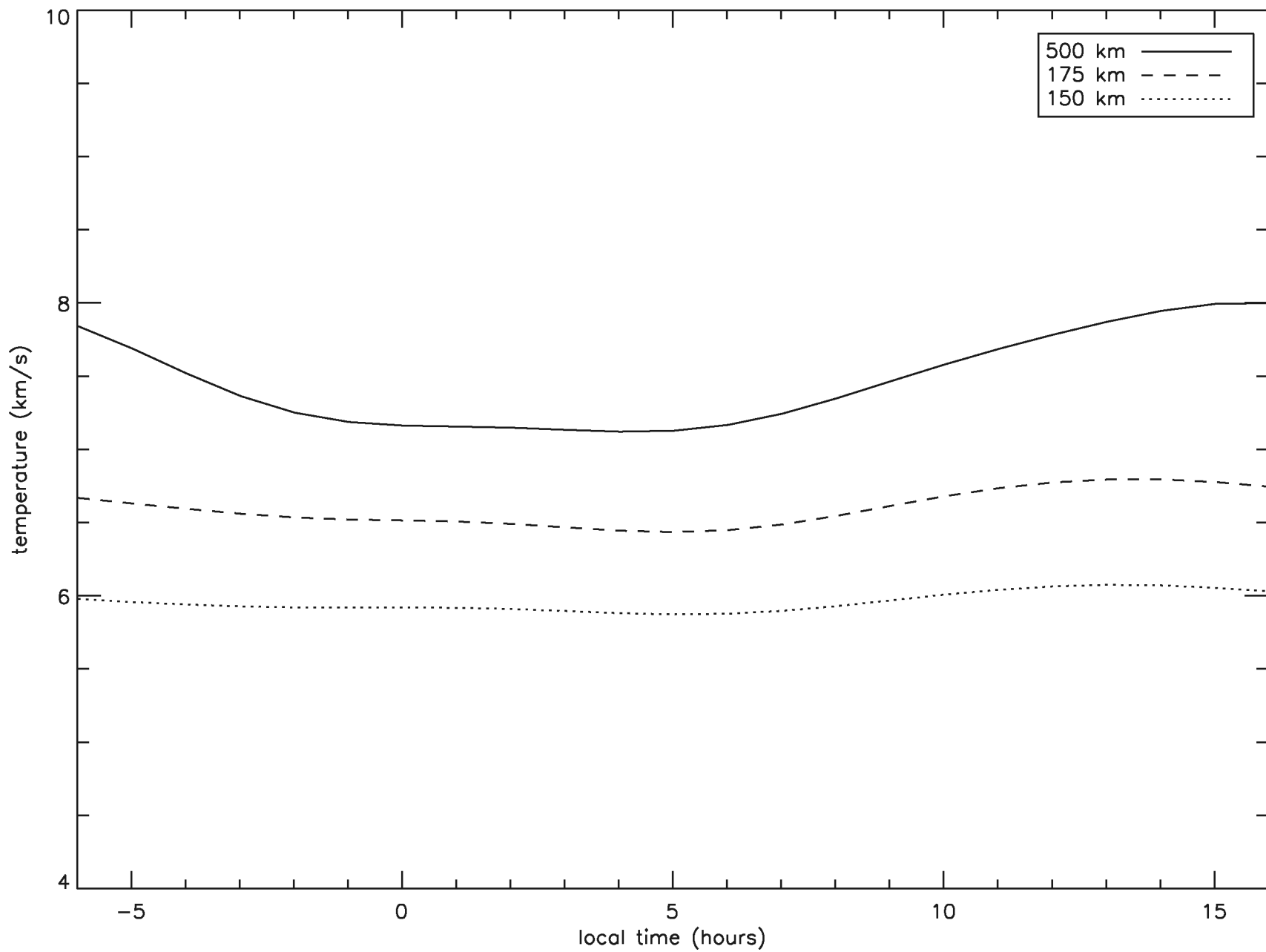
At about the same time as the NRL Lyman alpha (121.6 nm) detection, ground-based observers detected Balmer alpha (656.3 nm) in the night sky

– Balmer alpha "nightglow"
– the result of solar Lyman beta scattering
– Balmer alpha fluorescence ~12% of the time
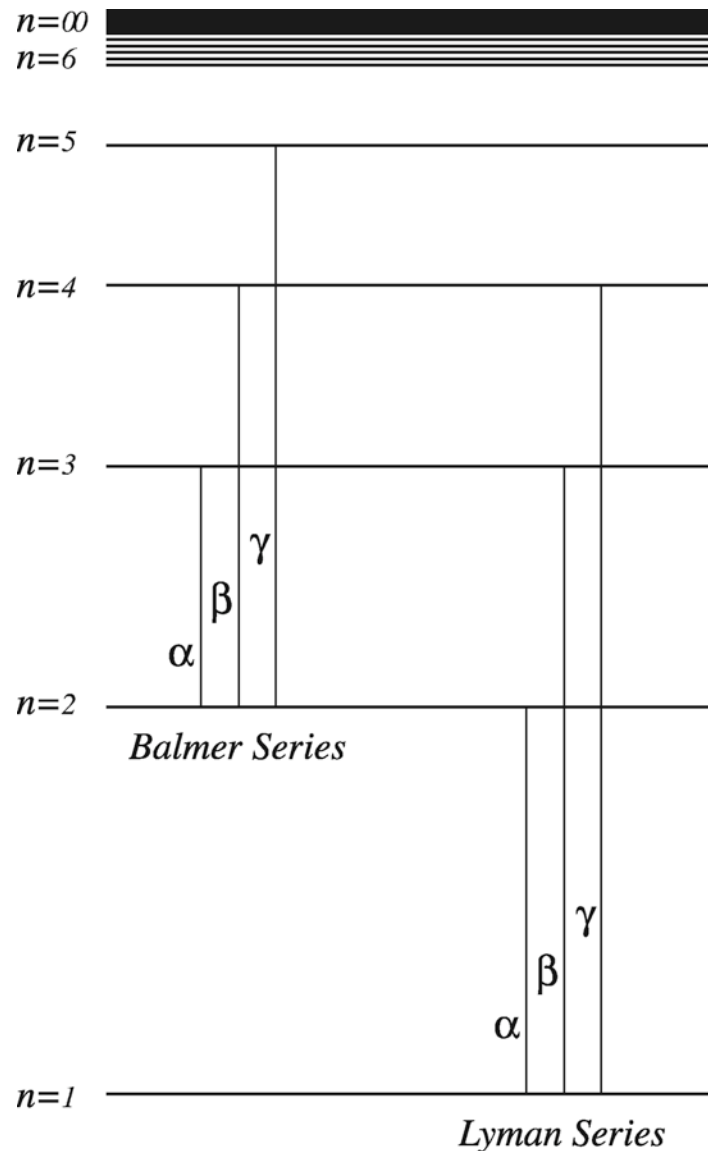
Concentration of Nightglow H_α-emission to the Ecliptic and the Radial Velocities of this Line

DURING the winter of 1962–63 I examined the distribution of H_α-intensity over the night sky. A Fabry-Pérot étalon was used with a spacing of 0·3 mm and reflexion coefficient 0·91 at H_α. An interference filter of 30 Å half-width was used as premonochromator. A contact image intensifier was used for registering the fringes. The whole system was installed on a small equatorial mounted in a tube in which temperature was controlled. The observations were made at the high-altitude station of the Sternberg Astronomical Institute ($\varphi = 44°$, $h = 3,000$ m) near Alma-Ata. One-hour exposure was sufficient to record H and OH fringes at any point of the sky, including the zenith.

The distribution of the night-glow H_α-emission shows a considerable concentration to the ecliptic and to the Sun. If the H_α intensity in the antisolar point is taken as 1, the intensity on the ecliptic at elongations 70°–90° from the Sun reaches 4–5 (Fig. 1). The distribution is markedly asymmetrical, the morning intensities being greater. The H_α intensity distribution across the ecliptic at the elongation of 90° (morning side) is shown in Fig. 2. The intensity of H_α in other point of the night sky at the same zenith distance, but far from the ecliptic, shows no enhancement. During the observations the regions close to the Sun were situated far from the Milky Way; its position is marked on Fig. 1. The H_α-intensity at 70°
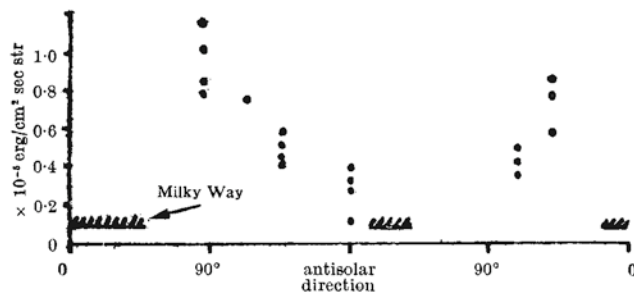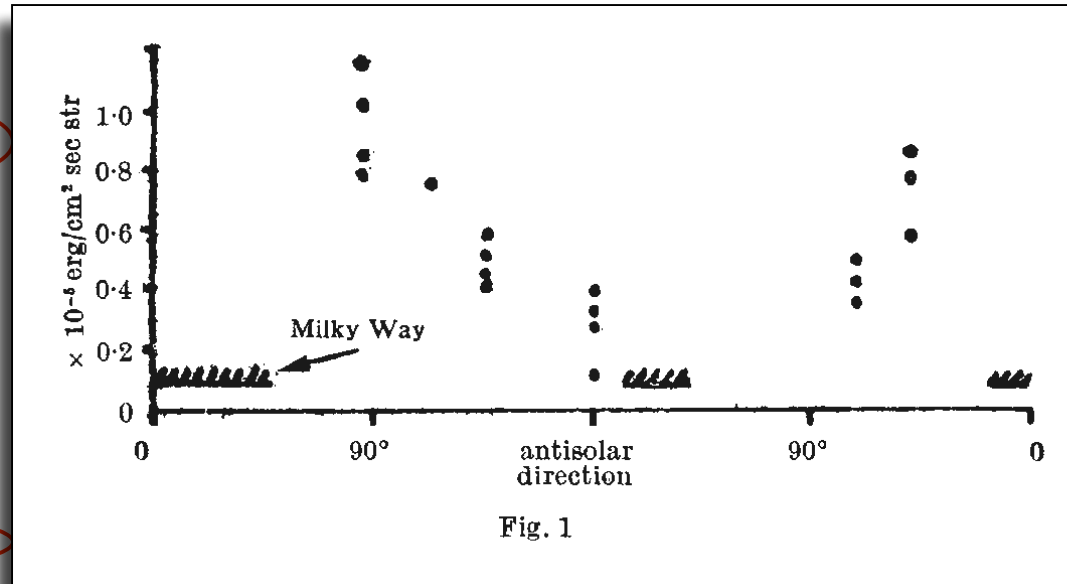

Fig. 1

value. In the antisolar direction a positive radial velocity was observed but not very certainly.

The small radial velocity and narrowness of the night-glow H_α line are strong arguments for its atmospheric origin. The observation can be fitted with the following model: neutral hydrogen forms a disk in the ecliptic plane 5,000 km thick and extended up to 3,000 km in the evening and to 10,000 km in the morning. During the night the hydrogen exosphere becomes denser as shown in a recent paper of Donahue (private communication). At sunrise intense dissipation begins, but the density remains high enough during several hours. It is a plausible explanation of the east–west asymmetry of the H_α night-glow. Such measurements can be used for determining the density of the exosphere, which depends strongly on the temperature of the thermopause. An interesting observational problem is the interaction of the Doppler-shifted Fraunhofer line in the zodiacal light and the H_α night-glow when observed with finite spectral resolving power. We have perhaps observed a darkening of the emission line at elongation near 90° due to such interaction.

P. V. SHEGLOV

Sternberg Astronomical Institute,
Moscow.

Fabry-Perot, Michelson, SHS

high throughput interference spectroscopy

- Throughput advantage over grating devices
  - ability to pass a large solid angle of light into a small spectral interval
- The crux of the issue:
  - Grating: $\lambda \propto \sin\theta \, (\sim\theta)$
  - Fabry-Perot: $\lambda \propto \cos\theta \, (\sim\theta^2)$
- For a given spectral interval $\delta\lambda$ a much larger opening angle $\delta\theta$ is allowed for the Fabry-Perot (Michelson or SHS)

Time or shadow altitude

NASA, Galileo spacecraft
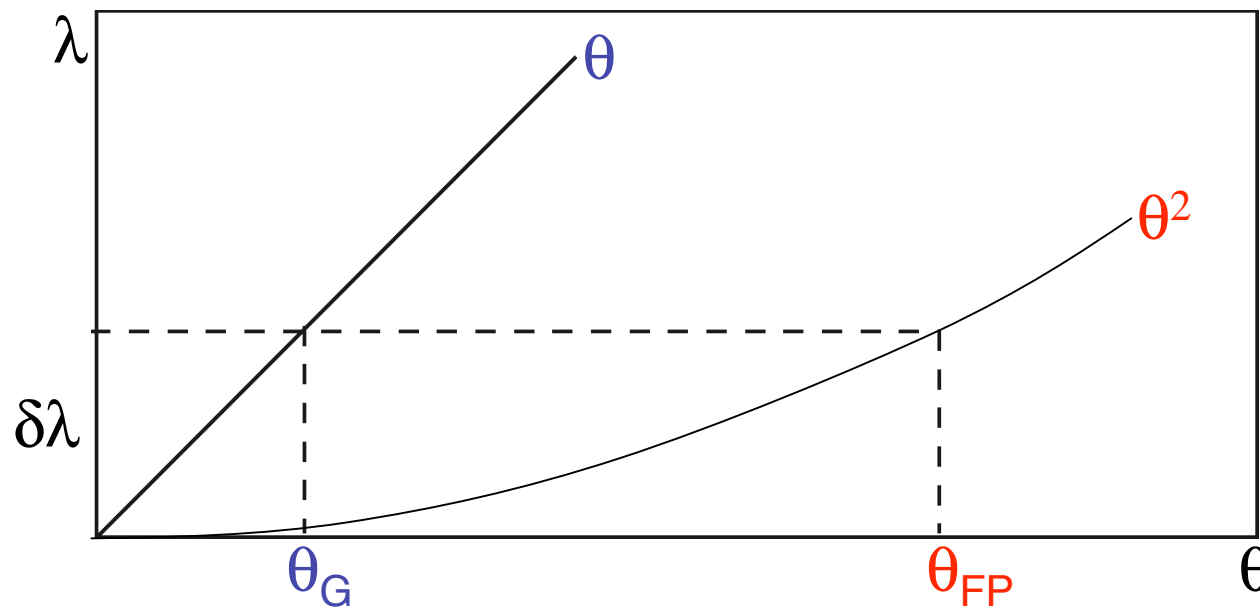
High-Resolution/High-Throughput Spectroscopy
a powerful tool to study the WIM (and the geocorona!)

LOW-INTENSITY BALMER EMISSIONS FROM THE
INTERSTELLAR MEDIUM AND GEOCORONA

R. J. REYNOLDS*
NASA, Goddard Space Flight Center, Greenbelt, Maryland

AND

F. L. ROESLER AND F. SCHERB
Physics Department, University of

Received 1972 June 12; revise

ABSTRACT

Galactic and nongalactic components of the diffuse
resolved with a Fabry-Perot spectrometer. The nongala
most of the emission at galactic latitudes greater than 30°
yield values for the average ionization rate per hydrogen a

I. INTRODUCTIO

A study of faint, diffuse galactic Hα and Hβ
150 mm diameter pressure-scanned Fabry-Perot
the 36-inch (91-cm) telescope at Goddard Spac
spectrometer has a spectral resolving power of 2
field of view. Faint Hβ emissions that do not appe
H II regions have previously been observed by Joh
and by Daehler *et al.* (1968) and Reay and Ring
meters; but low spectral resolution prevented them from using radial-velocity shifts
to discriminate between galactic and possible local emission sources. Since the galactic
hydrogen often has radial velocities of ± 25 km s^{-1} or more with respect to the Earth,
it has been possible with the present spectrometer's 12 km s^{-1} resolution to resolve the
unshifted (probably geocoronal) Hα and Hβ lines from the galactic lines, and thus
unambiguously determine for a variety of observation directions the relative contri-
butions of each source to the line intensities.
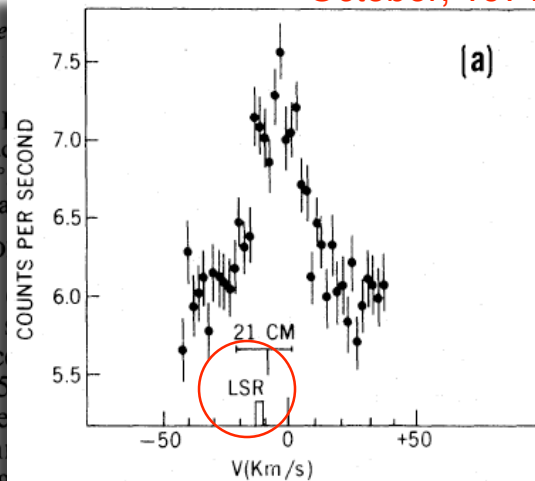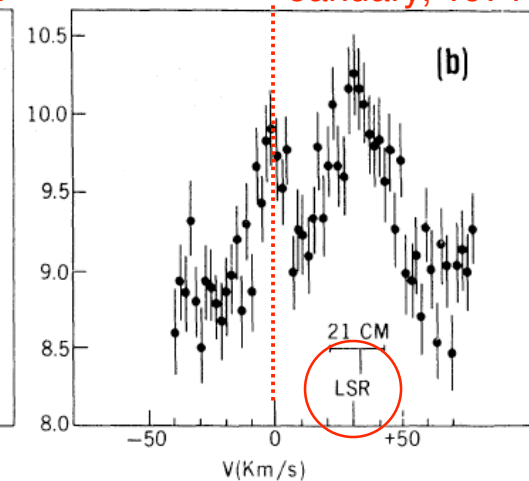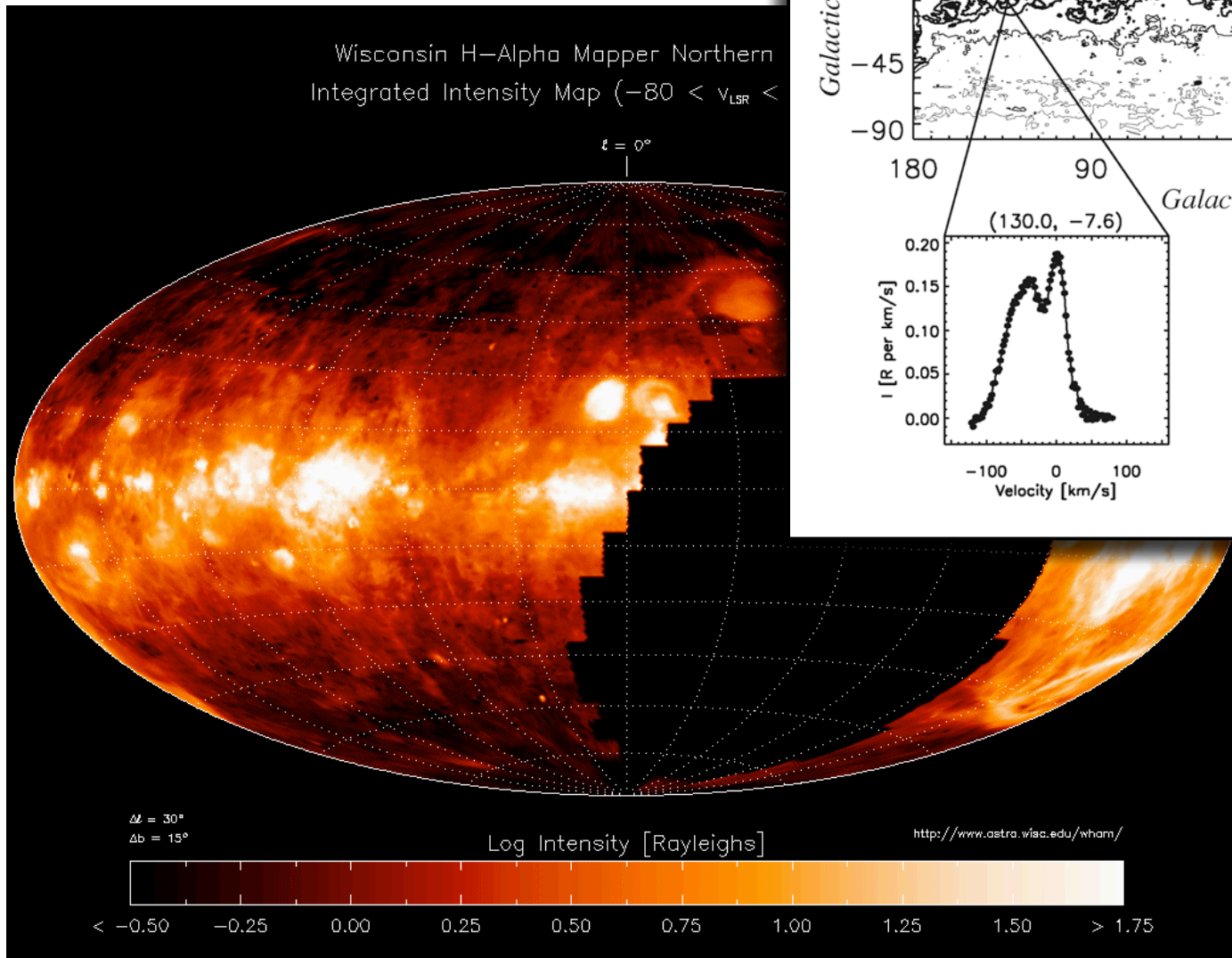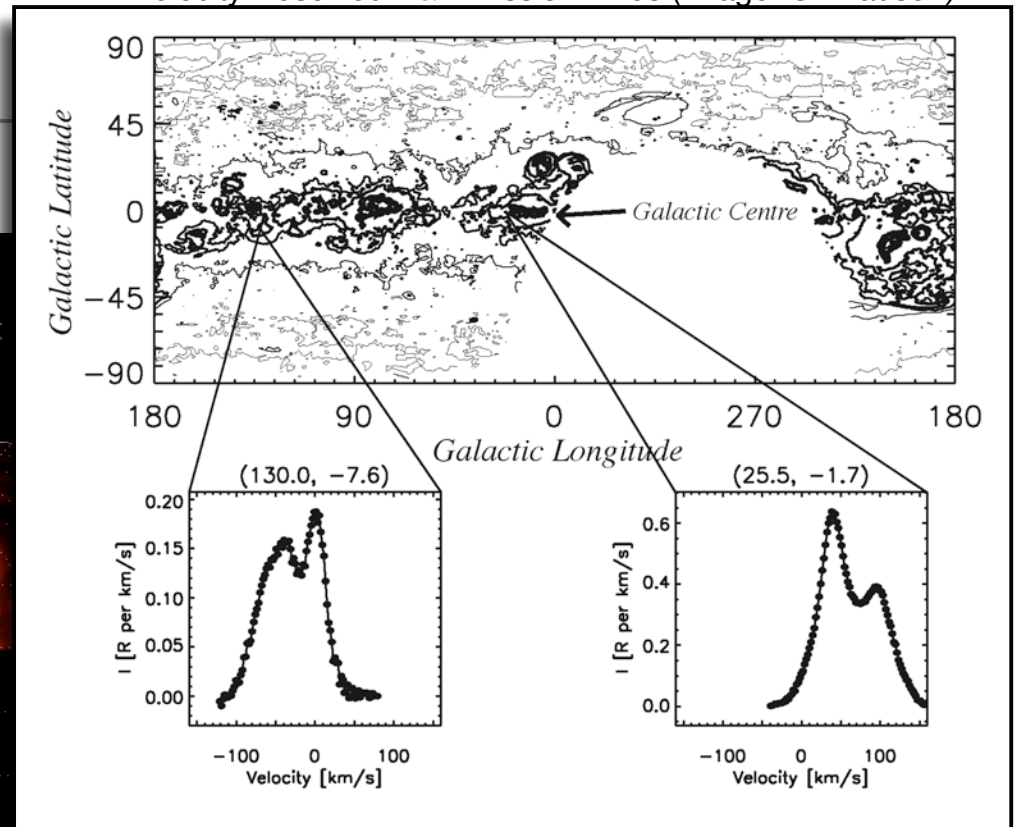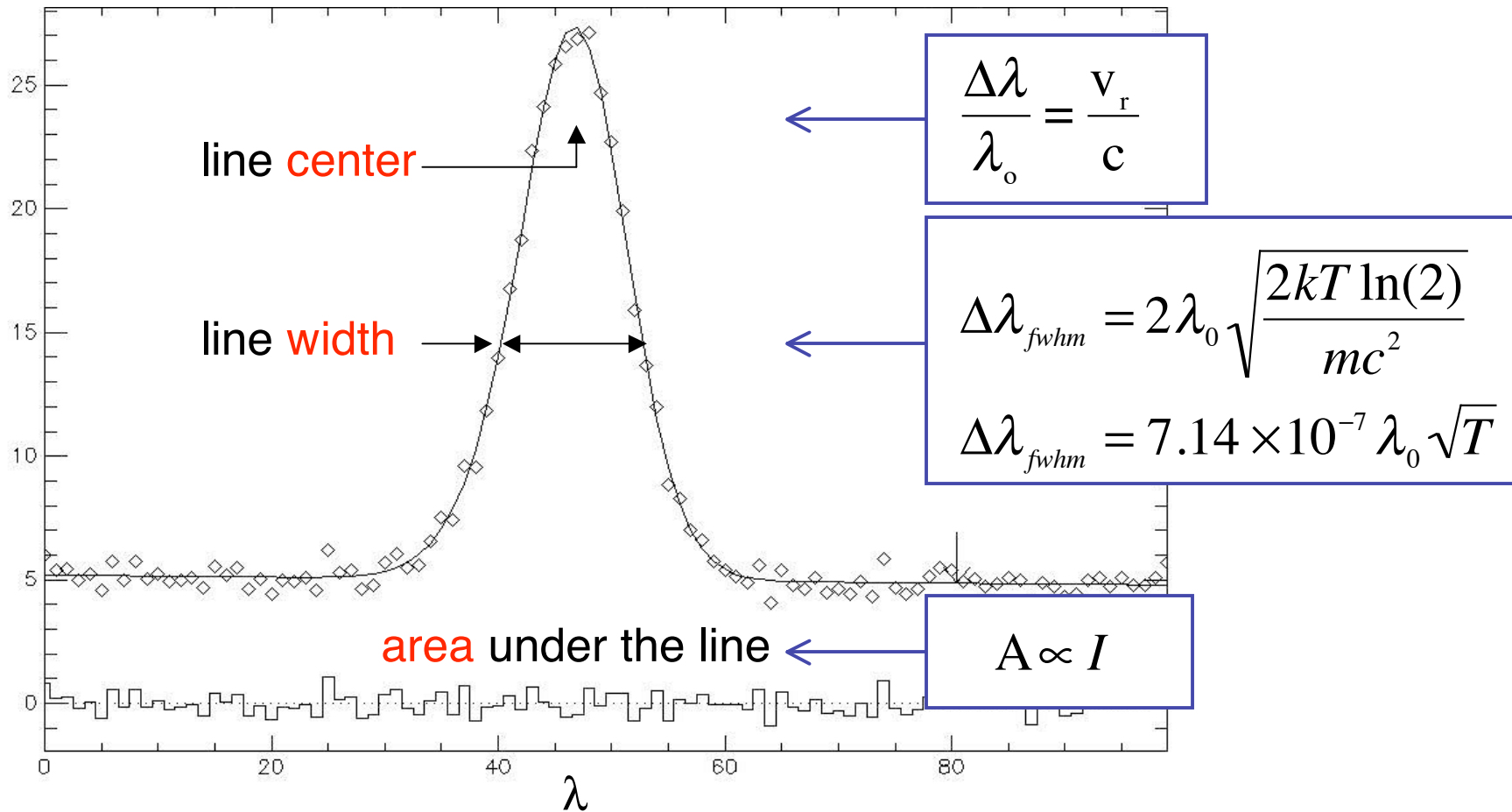
$$\frac{\Delta\lambda}{\lambda_o} = \frac{v_r}{c}$$

Velocity Resolved Hα Emission Lines (Image: *G. Madsen)*

Line Profile

$$\frac{\Delta\lambda}{\lambda_o} = \frac{v_r}{c}$$

$$\Delta\lambda_{fwhm} = 2\lambda_0 \sqrt{\frac{2kT\ln(2)}{mc^2}}$$

$$\Delta\lambda_{fwhm} = 7.14 \times 10^{-7} \lambda_0 \sqrt{T}$$

$$A \propto I$$

line center

line width

area under the line

MEASUREMENTS OF THE SPECTRAL PROFILE OF BALMER ALPHA EMISSION FROM THE HYDROGEN GEOCORONA

J. W. Meriwether, Jr., S. K. Atreya and T. M. Donahue

Space Physics Research Laboratory, Depa...
and Oceanic Science, The University of Michigan,

R. G. Burnside
Department of Physics, University...
Rio Piedras, Puerto Rico

Abstract. Instrumental improvements responsible for a factor of 25 increase in the sensitivity of the Fabry-Perot interferometer enable us to observe for the first time the short wavelength depletion of the Balmer α spectral profile due to hydrogen escape. These results are shown to be consistent with the implications of OGO-5 observations by Bertaux.

INTRODUCTION

Because the geocorona is optically thin at the wavelength of the atomic hydrogen Balmer alpha (Hα) emission line at 6562.8Å, ground-based observations at high spectral resolution of the spectral profile of Hα, produced by hydrogen fluorescence of Lyman β photons, are linked directly to measurements of the velocity distribution of hydrogen atoms. *Chamberlain* [1976] and *Prisco and Chamberlain* [1978; 1979] have made extensive calculations concerning the expected shape for the zenith orientation, but the predicted departures from the Maxwellian profile are small and difficult to observe. The first observations of the Hα spectral profile at high resolution were made by *Atreya* et al. [1975] with a Fabry-Perot interferometer of low sensitivity (0.05 counts/secR). By averaging all observations obtained each night, values for the apparent thermal width were found to lie in the range between 700 and 850K.

firmed...
The be...
a facto...
maxim...
tamina...
sensiti...

In t...
a serio...
The ex...
a sma...
galacti...
tions a...
identif...
would...
of the...
the rer...
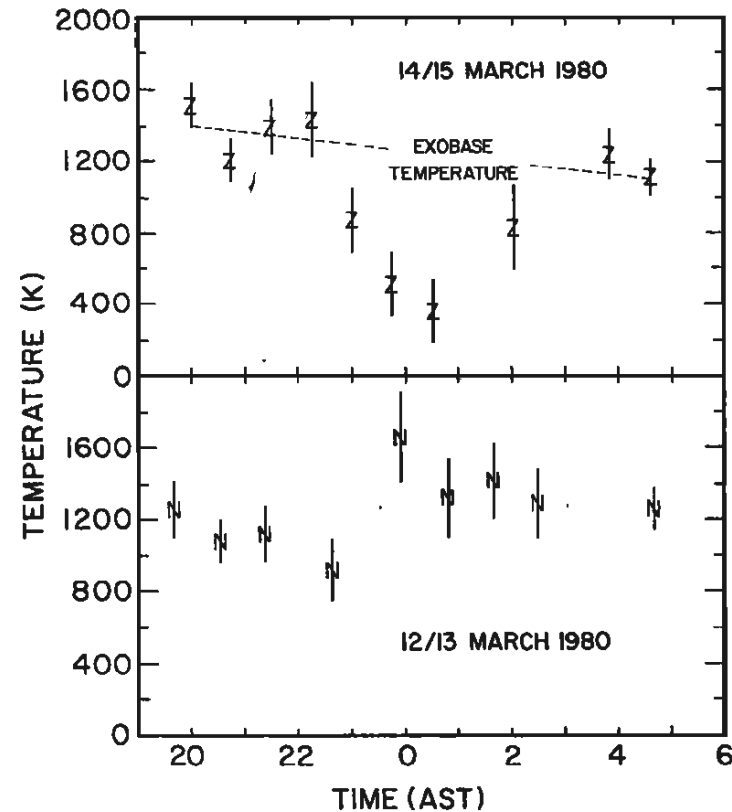set.

The...
interfe...
applica...
impro...
is redu...
Cali...

Fig. 4. Temperature plots deduced from apparent thermal width of Hα for 12/13 March and 14/15 March, 1980. Temperature error bars span ± 2 standard deviations.
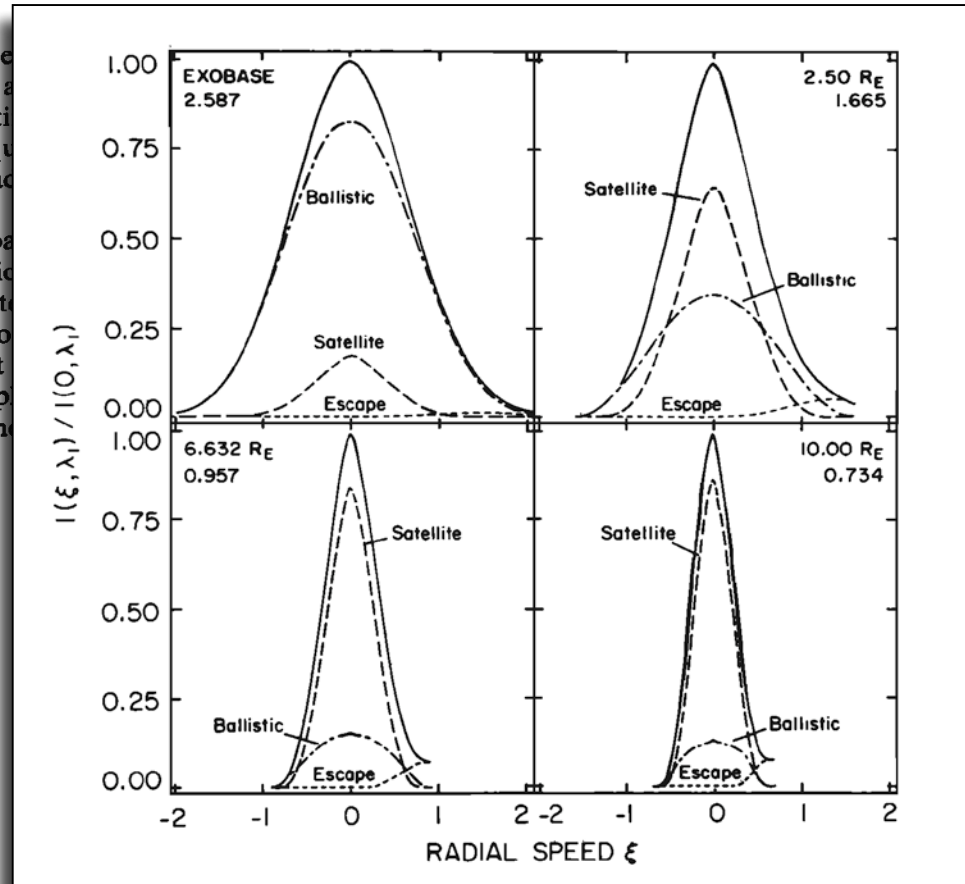
Geocoronal Structure
3. Optically Thin, Doppler-Broadened Line Profiles

JAMES BISHOP AND JOSEPH W. CHAMBERLAIN

Department of Space Physics and Astronomy, Rice University, Houston, Texas

Theoretical line profiles, applicable to the
ed for illustrative cases. While retaining
equilibrium plasmasphere conditions), disti
corona are isolated. Examining the consequ
here. In the prototype evaporative case, ra
of an extensive quasi-satellite component.
theory discloses the influence of an exopa
spectral shapes in the geocoronal applicatic
(1) a blueward "shift" or bias near line cent
by loss mechanisms acting over the time o
tion) and (2) an enhanced redward wing at
height escape speed, produced by plasmasp
for recent observations of geocoronal H$_\alpha$ lin

Geocoronal Structure, 2. Inclusion of a Magnetic Dipolar Plasmasphere

James Bishop
Department of Space Physics and Astronomy, Rice University, Houston, Texas

Joseph W. Chamberlain
Department of Space Physics and Astronomy, Rice University, Houston, Texas

Calculations of exospheric quantities (hydrogen atom ... kinetic temperature, and escape flux) at locations alo... midnight directions have been extended to incorpora... shape and an empirical temperature profile. This inter... corresponding to low-to-moderate solar conditions, r... geocoronal positions; the effect is not dramatic, thou... evaporative case closely, in spite of the control of tra... collisions. A careful discussion of the handling of pla... solar ionization is included, and the effect on the exo... terms of pertinent examples. In addition, the geotail i... imposition of an exopause by radiation pressure dyna...

Citation: Bishop, J., and J. Chamberlain (1987), Geocorona... Plasmasphere, J. Geophys. Res., 92(A11), 12377-12388.

Geocoronal Structure: The Effects of Solar Radiation Pressure and the Plasmasphere Interaction

James Bishop
Department of Space Physics and Astronomy, Rice University, Houston, Texas

The theory of planetary exospheres is extended to incorporate solar radiation pressure in a rigorous manner, and an evaporative geocoronal prototype (classical, motionless exobase) is constructed using Liouville's theorem. Model calculations for density and kinetic temperature at points along the earth-sun axis (solar and antisolar directions) reveal an extensive satellite component, comprising ~2/3 of the total hydrogen density near 10 earth radii, and a temperature profile suggestive of an isotropic quasi-Maxwellian velocity distribution for the bound component. A geotail is also evident as an enhancement of the density at local midnight compared to local noon that increases outward (from ~25% at 10 earth radii to over 60% at 20 earth radii). Additional mechanisms acting upon the geocorona alter the basic evaporative case in notable ways. Solar ionization has been included in a simple fashion; the effect is to partially deplete the density without otherwise altering the structure. Interaction with a simple plasmasphere via the Boltzmann equation results in "heating" the geocorona and enhancing the escape flux at the expense of the density of the bound component, an effect not appreciated in earlier studies; the geotail survives this interaction.

Citation: Bishop, J. (1985), Geocoronal Structure: The Effects of Solar Radiation Pressure and the Plasmasphere Interaction, J. Geophys. Res., 90(A6), 5235-5245.

PBO and WHαM
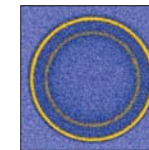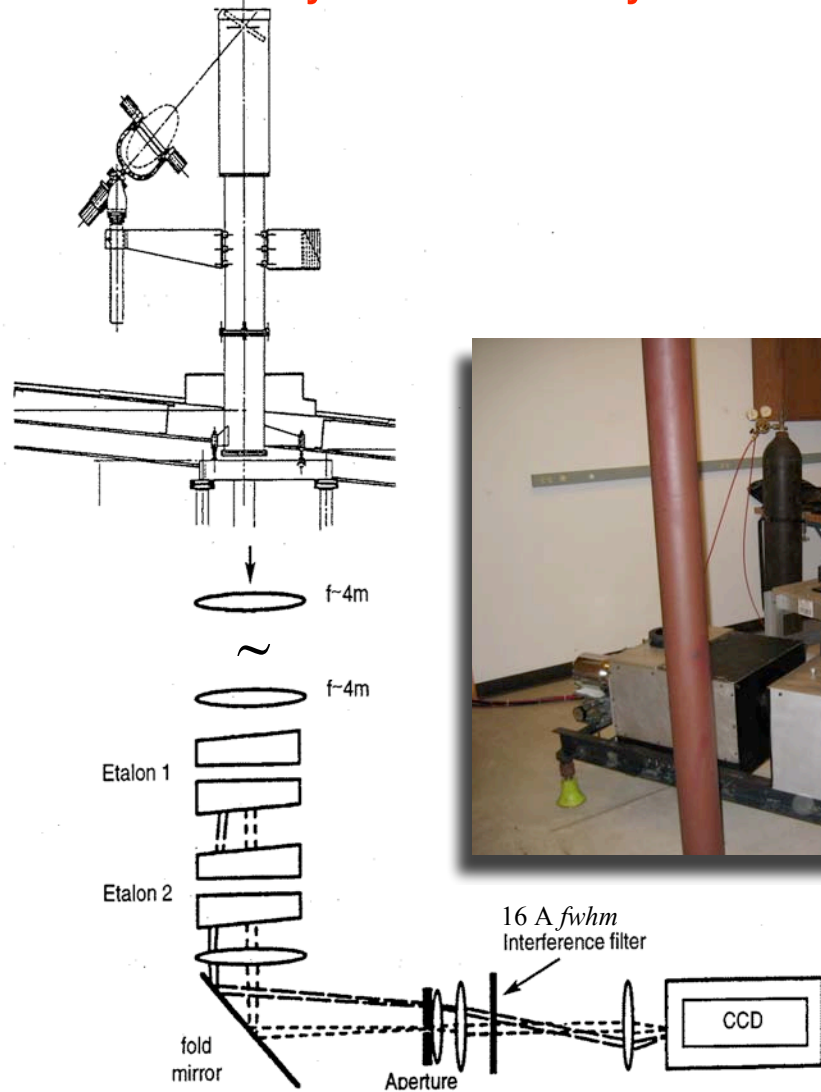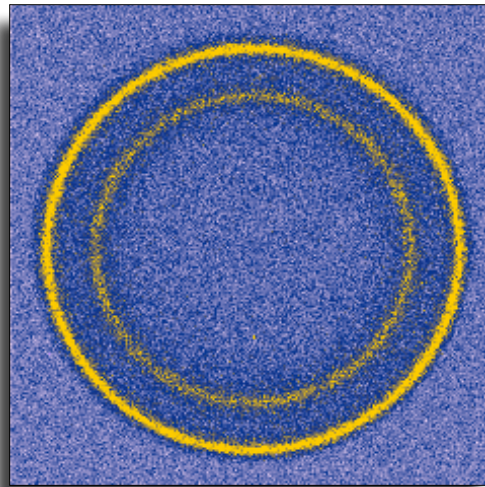## for Aeronomy & Astronomy

Photo: *C. Anderson*

PBO and WHαM

for Aeronomy & Astronomy

f~4m

~

f~4m

Etalon 1

Etalon 2

16 A *fwhm*
Interference filter

fold mirror

Aperture

CCD

PBO and WHαM

for Aeronomy & Astronomy

WHαM

PBO
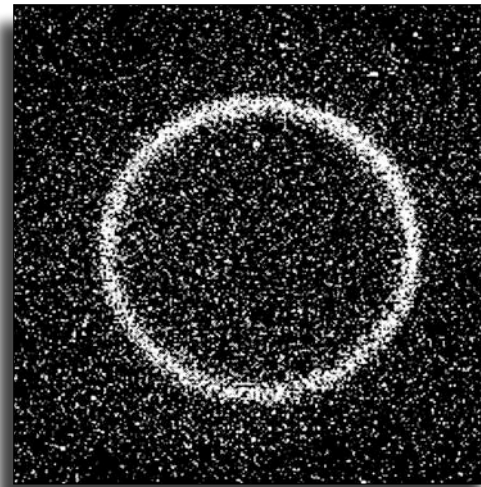
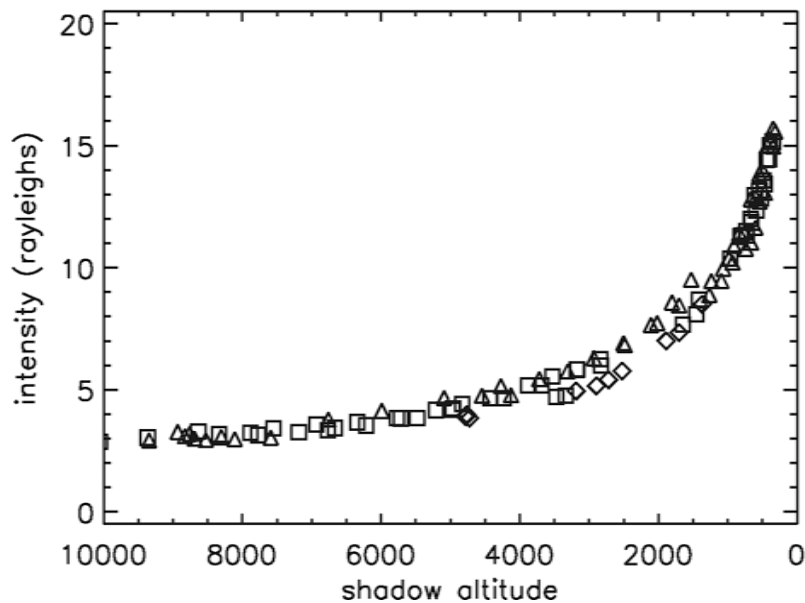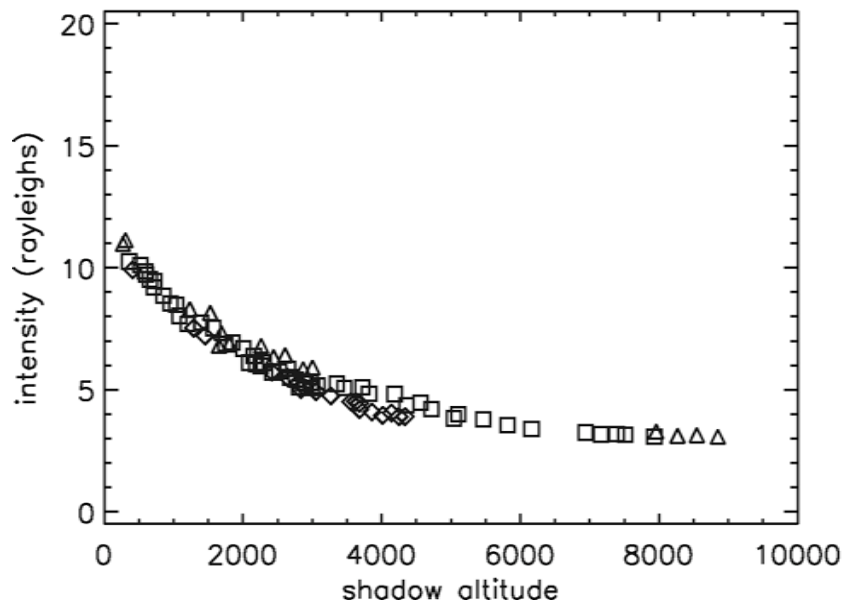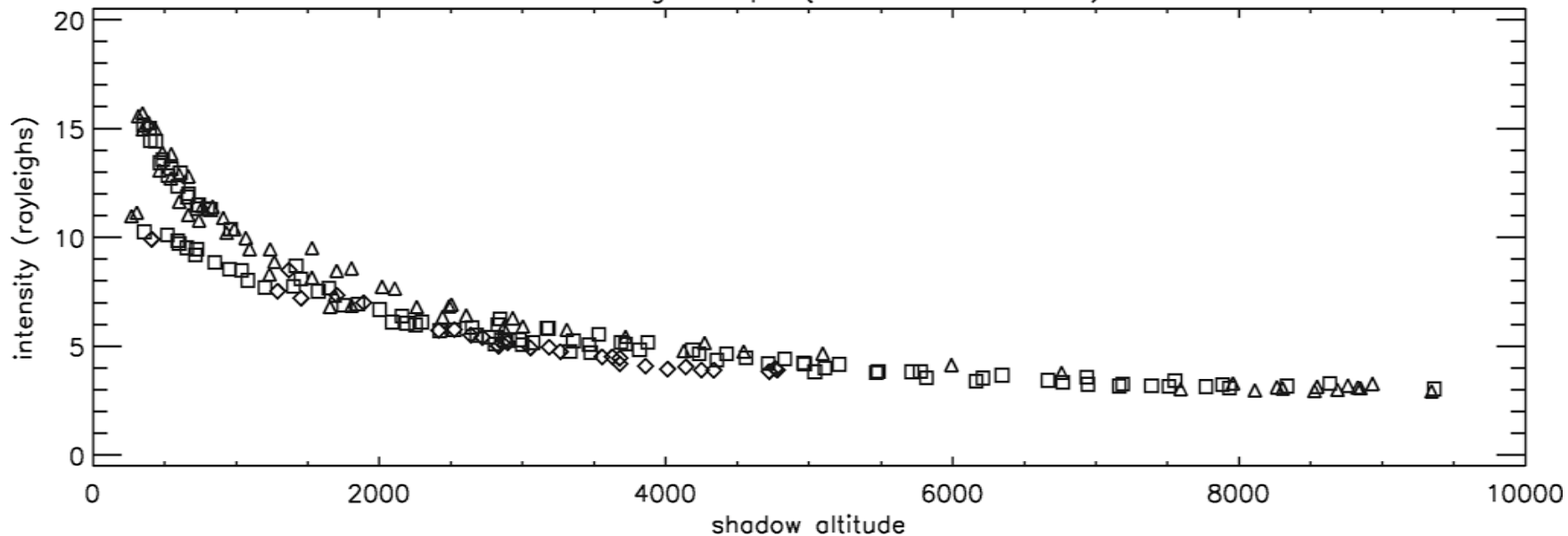200 km/s

4500-9000 A

12 km/s (R~25,000)

1° beam

75 km/s

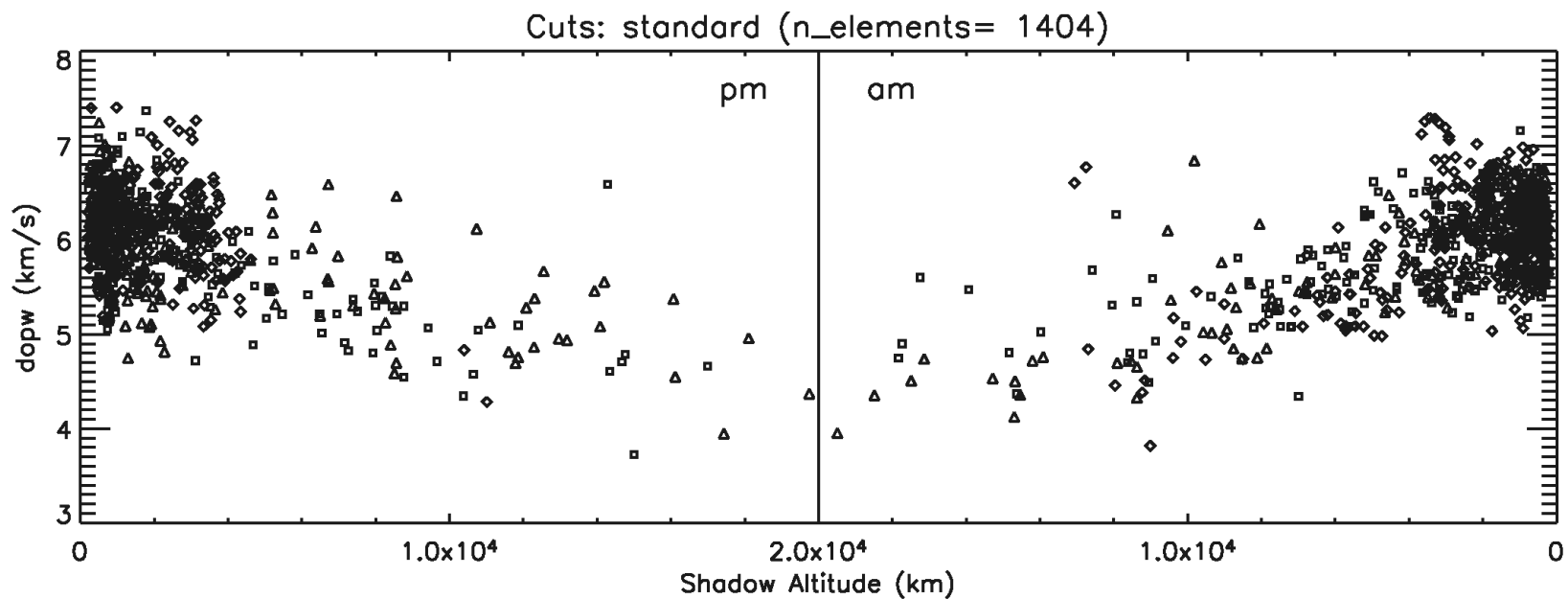4500-9000 A

3.75 km/s (R~80,000)

1.5° beam

series2_igeo_d.ps (n_elements= 212)

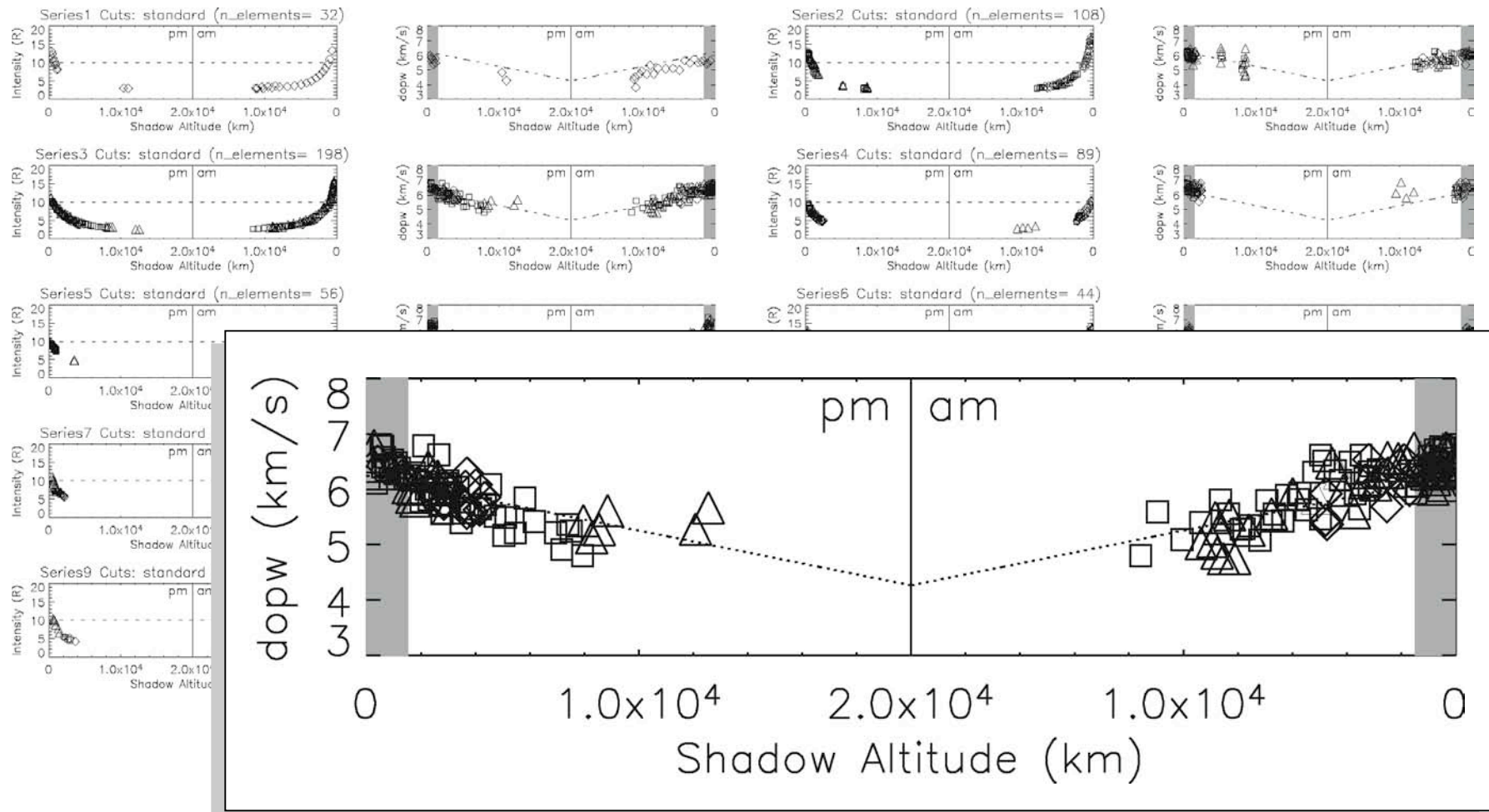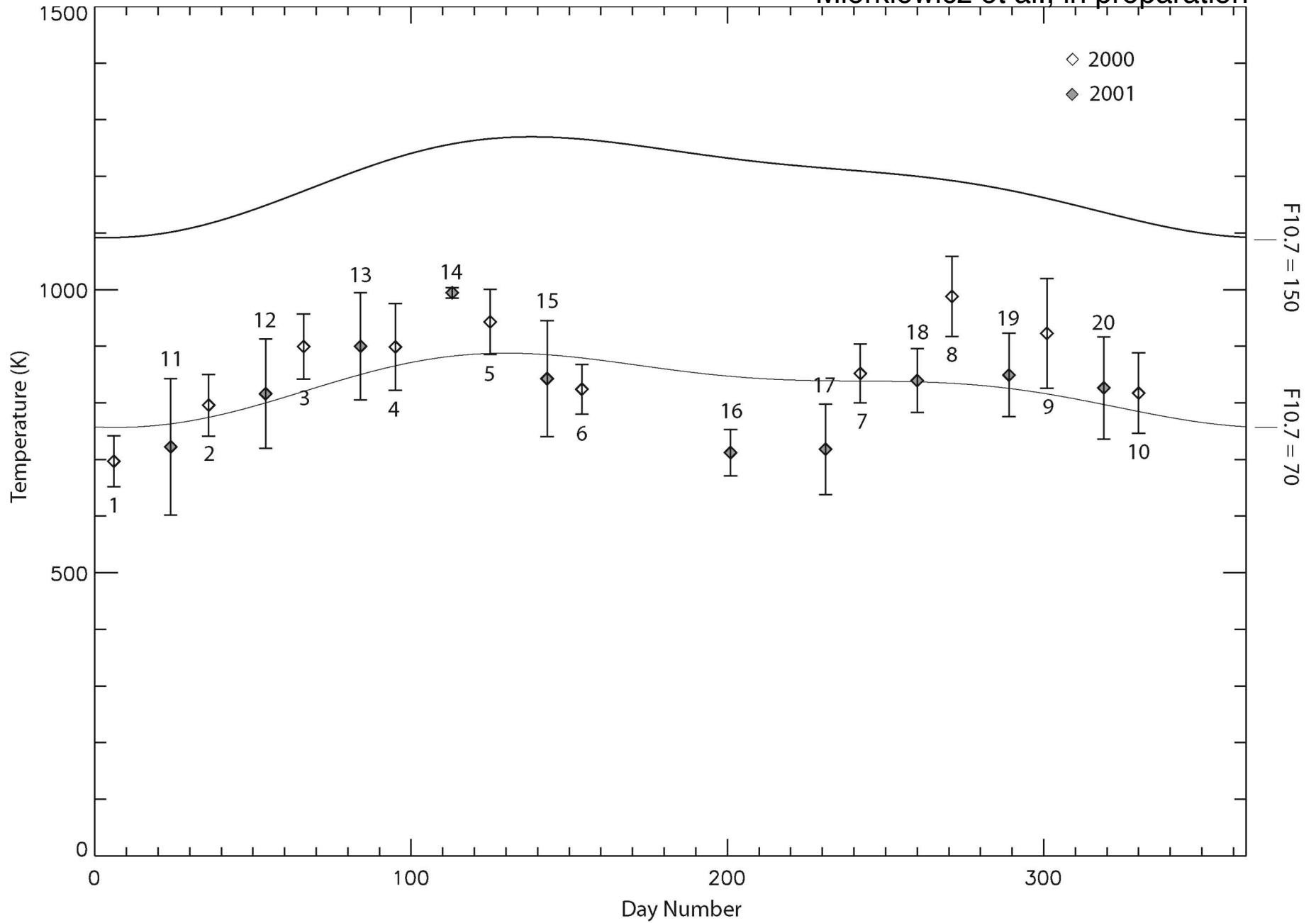Cuts: standard (n_elements= 1404)

In terms of T_{eff} ~500 K decrease from ~850 K @ 500 km to ~350 K @ 20,000 km

PBO 2000-2001

Mierkiewicz et al., in preparation

The Earth's Hydrogen Corona   Mierkiewicz, CEDAR 2010

Pergamon

TRANSPORT OF RESONANT ATOMIC HYDROGEN EMISSIONS IN THE THERMOSPHERE AND GEOCORONA: MODEL DESCRIPTION AND APPLICATIONS

JAMES BISHOP

Computational Physics Incorporated, Fairfax, VA 22031, USA

Abstract—A computer code for calculating global models of atomic hydrogen Lyman series volume excitation rates and line-of-sight radiances has been developed for upper atmospheric modeling and remote sensing data analyses. It is based on the Anderson–Hord algorithm for solving the integral form of the transport equation and rigorously accounts for nonisothermal and pure absorption effects within the complete frequency redistribution approximation. Preliminary variants of the code have been in use by several groups for several years, and a fully tested version is now available for distribution. In this paper, the method for solving the transport equation is briefly reviewed and the key parameters identified. Validation of the code is illustrated via comparisons with previously analyzed data sets: STP 78-1 EUV spectrometer limb profiles and geocoronal "images" obtained with the UV imaging photometer on DE-1. © 1999 Elsevier Science Ltd. All rights reserved.

Analysis of Balmer α intensity measurements near solar minimum

J. Bishop[a,*], J. Harlander[b], S. Nossal[c], F.L. Roesler[c]

[a] E.O. Hulburt Center for Space Research, Naval Research Laboratory, Code 7643, 4555 Overlook Avenue,
SW, Washington, DC 20375-5320, USA
[b] St. Cloud State University, St. Cloud, MN, USA
[c] University of Wisconsin-Madison, Madison, WI, USA

Abstract

Balmer α intensity measurements made with a dual etalon Fabry–Perot spectrometer at Haleakala during two campaigns in 1988 are presented. The data from each campaign demonstrate night-to-night stability, despite variations in geophysical conditions. Analysis of these data using a nonisothermal Lyman β radiative transport code, updated solar Lyman β line-center flux estimates, and corrected thermospheric atomic hydrogen density profiles points to the resolution of the "factor of 2" problem. A careful reassessment of other mechanisms for upper atmospheric Balmer α excitation has also been carried out.

Radiative transport code: lyao_rt

- lyao_rt (*Bishop*, 1999)
  - Spherically symmetric non-isothermal atmosphere
  - Generates global source functions & ACERs (intensities)
- lyao_rt and $H(z)$
  - Bishop's 3-parameter diffusive flow algorithm (*Bishop*, 2001)
  - Exobase density $[H]_c$
    - Mesospheric peak density $[H]_{peak}$
    - Photochemically initiated upward flux $\phi(H)$
    - MSIS background atmosphere
      - $T(z)$, $[O](z)$, $[N_2](z)$ and $[O_2](z)$ profiles
    - Extension of H to exosphere *via* analytic geocorona of *Bishop* (1991) $(T_s$ and $n_s)$
      - or evaporative case
      - or Chamberlain model (r_c)

The Earth's Hydrogen Corona — Mierkiewicz, CEDAR 2010

Radiative transport code: lyao_rt

Nossal et al., in preparation

WHAM 2000 Int/LYAO MSIS00 Max
WHAM 2006 Int/LYAO MSIS00 Min
WHAM 2000 Int/LYAO TGCM Max
WHAM 2006 Int/LYAO TGCM Min

Solar Cycle Comparison at 2800km

Nossal et al., in preparation
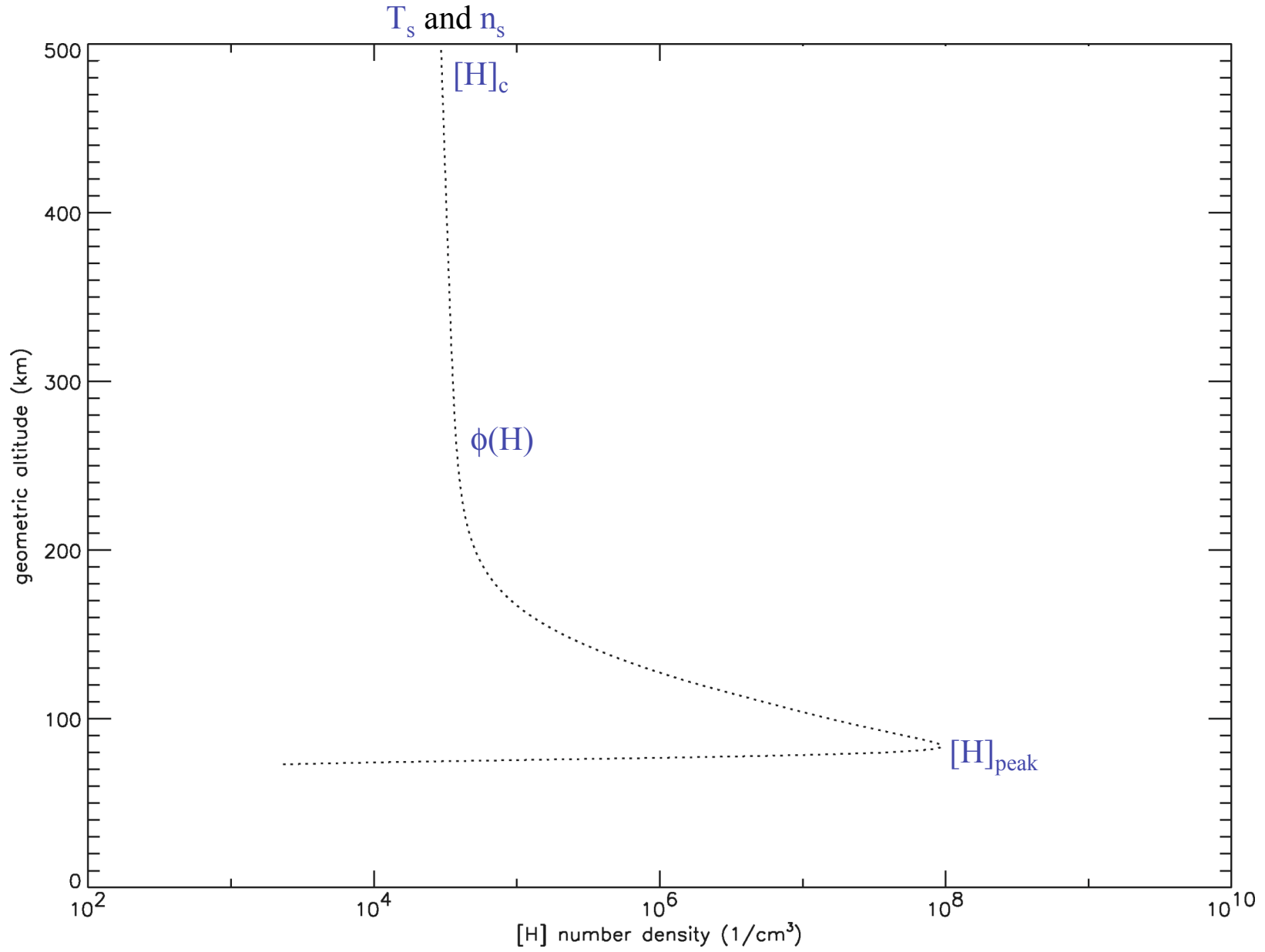
Radiative transport code: lyao_rt

our goal: map-out atomic hydrogen density distributions
from 100 - 20,000 km (and beyond)

- lyao_rt (*Bishop*, 1999)
  - Spherically symmetric non-isothermal atmosphere
  - Generates global source functions & ACERs (intensities)
- lyao_rt and $H(z)$
  - Bishop's 3-parameter diffusive flow algorithm (*Bishop*, 2001)
  - Exobase density $[H]_c$
    - Mesospheric peak density $[H]_{peak}$
    - Photochemically initiated upward flux $\phi(H)$
    - MSIS background atmosphere
      - $T(z)$, $[O](z)$, $[N_2](z)$ and $[O_2](z)$ profiles
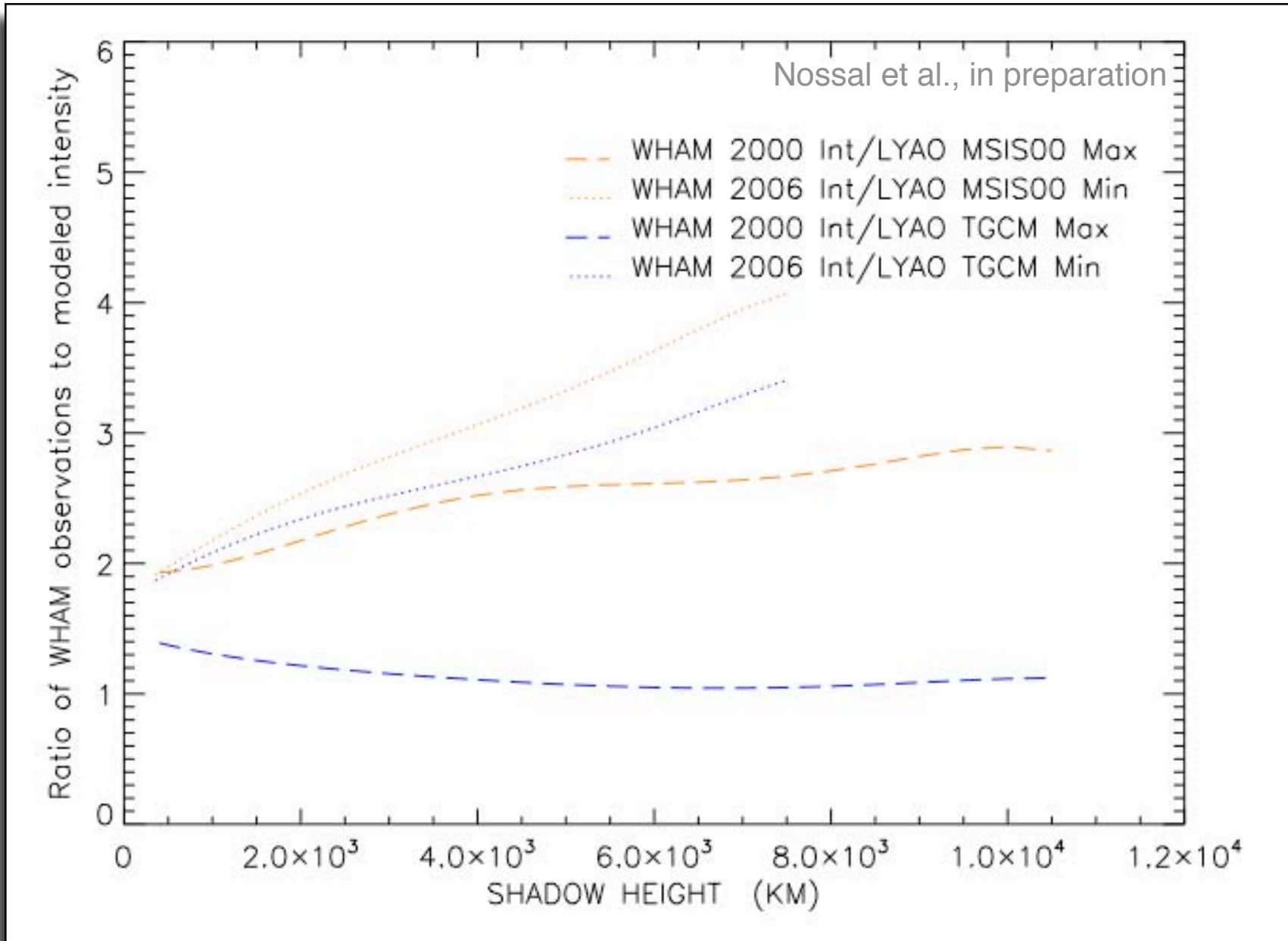   - Extension of H to exosphere *via* analytic geocorona of *Bishop* (1991) $(T_s$ and $n_s)$
      - or evaporative case
      - or Chamberlain model (r_c)

*assess the degree to which these
parameters might be constrained*

Data-model comparison search analysis of coincident PBO Balmer α, EURD Lyman β geocoronal measurements from March 2000

J. Bishop

E. O. Hulburt Center for Space Research, Naval Research Laboratory, Washington, D. C., USA

E. J. Mierkiewicz and F. L. Roesler

Department of Physics, University of Wisconsin-Madison, Madison, Wisconsin, USA

J. F. Gómez and C. Morales

Laboratorio de Astrofísica Espacial y Física Fundamental, I

[1] Recent Lyman series and Balmer series airglow measurements provide a fresh opportunity to investigate the density distribution and variability of atomic hydrogen in the upper atmosphere. Dedicated nightside Balmer α Fabry-Perot spectrometer measurements at the Pine Bluff Observatory (PBO), University of Wisconsin-Madison, have been acquired since late 1999 taking advantage of several technological advances. Extreme ultraviolet spectral radiance measurements by the Espectrógrafo Ultravioleta extremo para la Radiación Difusa (EURD) instrument on the Spanish MINISAT-1 satellite from October 1997 to December 2001 provide extensive sets of geocoronal Lyman β, Lyman γ and He 584 Å emission intensities. In this paper, coincident EURD Lyman β and PBO Balmer α radiance measurements from the early March 2000 new moon period are presented. In addition to serving as examples of the data sets now available, the data volume poses an analysis challenge not faced in prior geocoronal studies. A data-model comparison search procedure employing resonance radiation transport results for extensive sets of parametric density distribution models is being developed for use in analyses of multiple large data sets; this is described, and example results for the PBO and EURD March 2000 data sets are presented. The tightness of the constraints obtained for the solar line-center Lyman β irradiance and the atomic hydrogen column abundance is somewhat surprising, given the crudeness of the parameter binning in the search procedure and the fact that a small number of recognized corrections remain to be made to each data set. INDEX TERMS: 0310 Atmospheric Composition and Structure: Airglow and aurora;

Parametric model database

PBO/EURD model parameters

The range of model parameters used in our search

Parameter	Grid
$[H]_c$	$2, 2.8, 4, 5.7, 8, 11.3 \times 10^4$ cm^{-3}
$\phi(H)$	$0.3, 1, 3, 9 \times 10^8$ cm^{-2} s^{-1}
$[H]_{peak}$	$0.3, 1, 3, 9 \times 10^8$ cm^{-3}
T_s	$450, 600, 750, 1100$ K
$f(n_s)$	$0.73, 1.0, 1.36$
$f(F_{10.7})$	$0.85, 1.0, 1.15$

- lyao_rt was run to generate an extensive set of source functions based on the parameters defined above
- LOS intensities were generated for each PBO/EURD pointing
- Model runs which replicated the variation of both the PBO/EURD data sets were selected

Parametric model search

PBO/EURD best fit
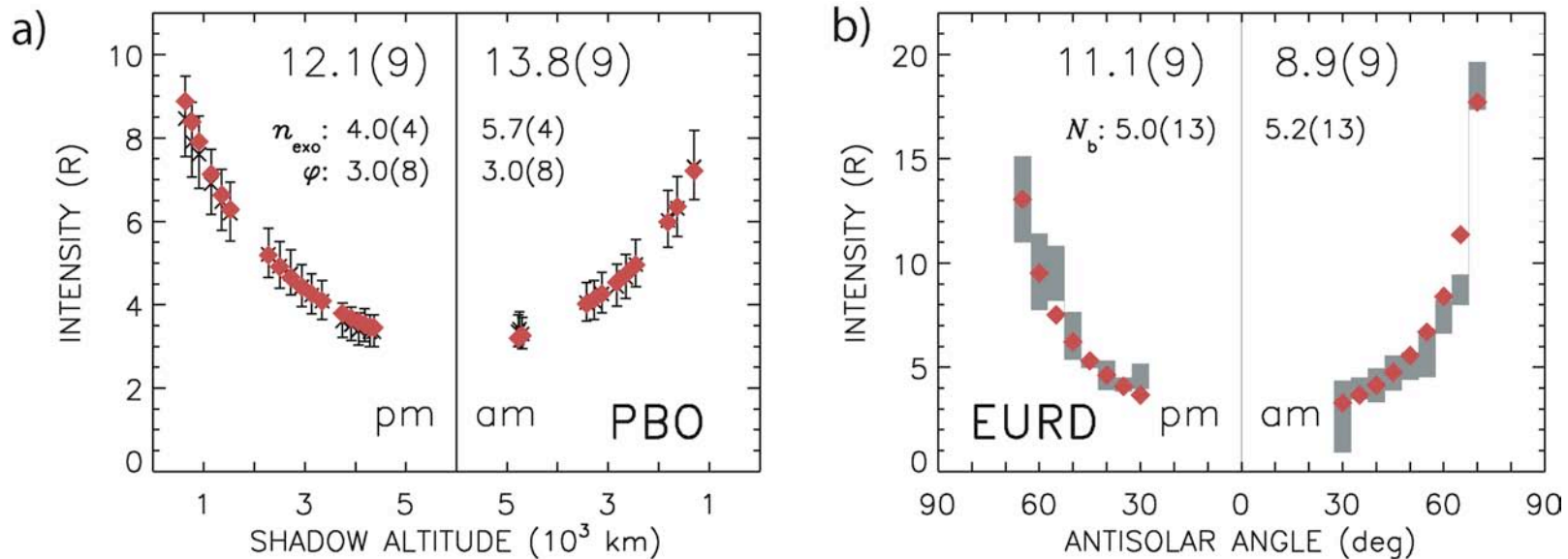
- lyao_rt was run to generate an extensive set of source functions based on the parameters defined above
- LOS intensities were generated for each PBO/EURD pointing
- Model runs which replicated the variation of both the PBO/EURD data sets were selected

MSIS Thermospheric [H](z) Profile

WHαM Hα/Hβ data (2008)
alternating blocks of Hα (30s) and Hβ (60s)

state of the art in the early *70s*

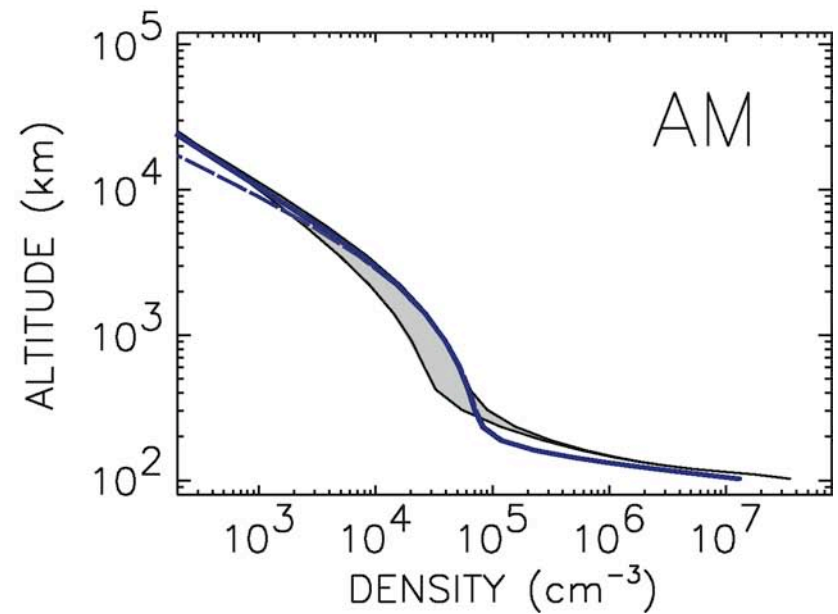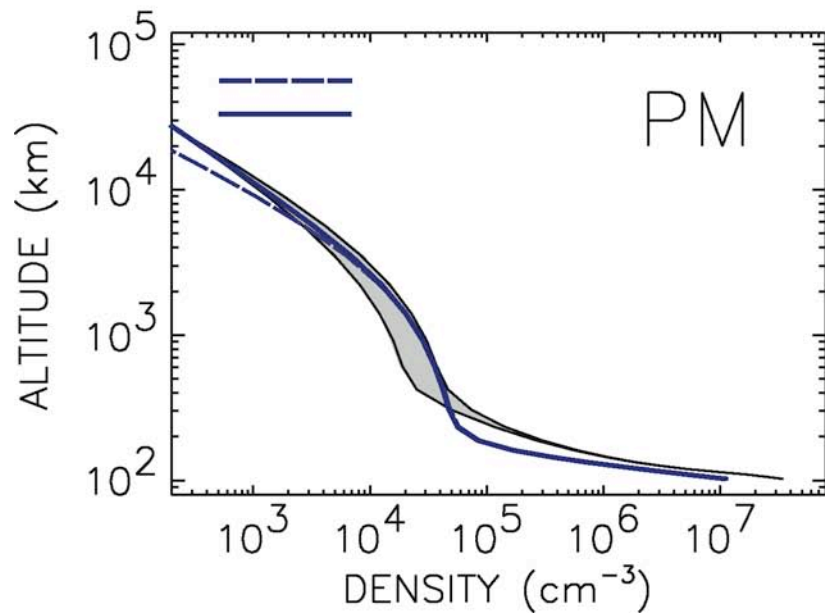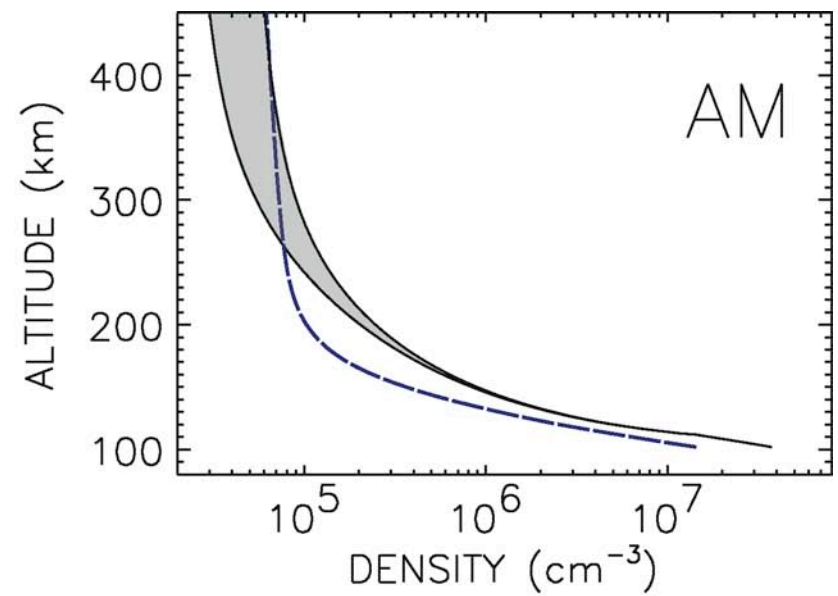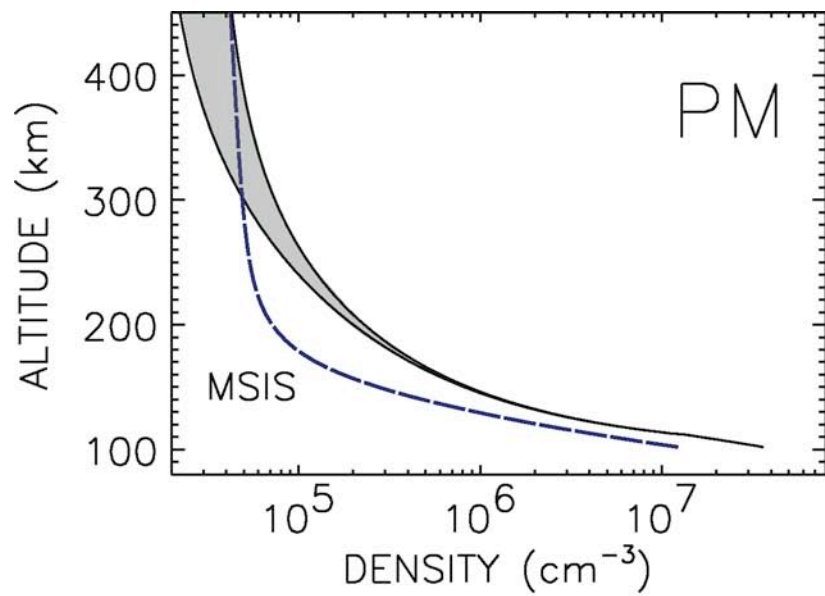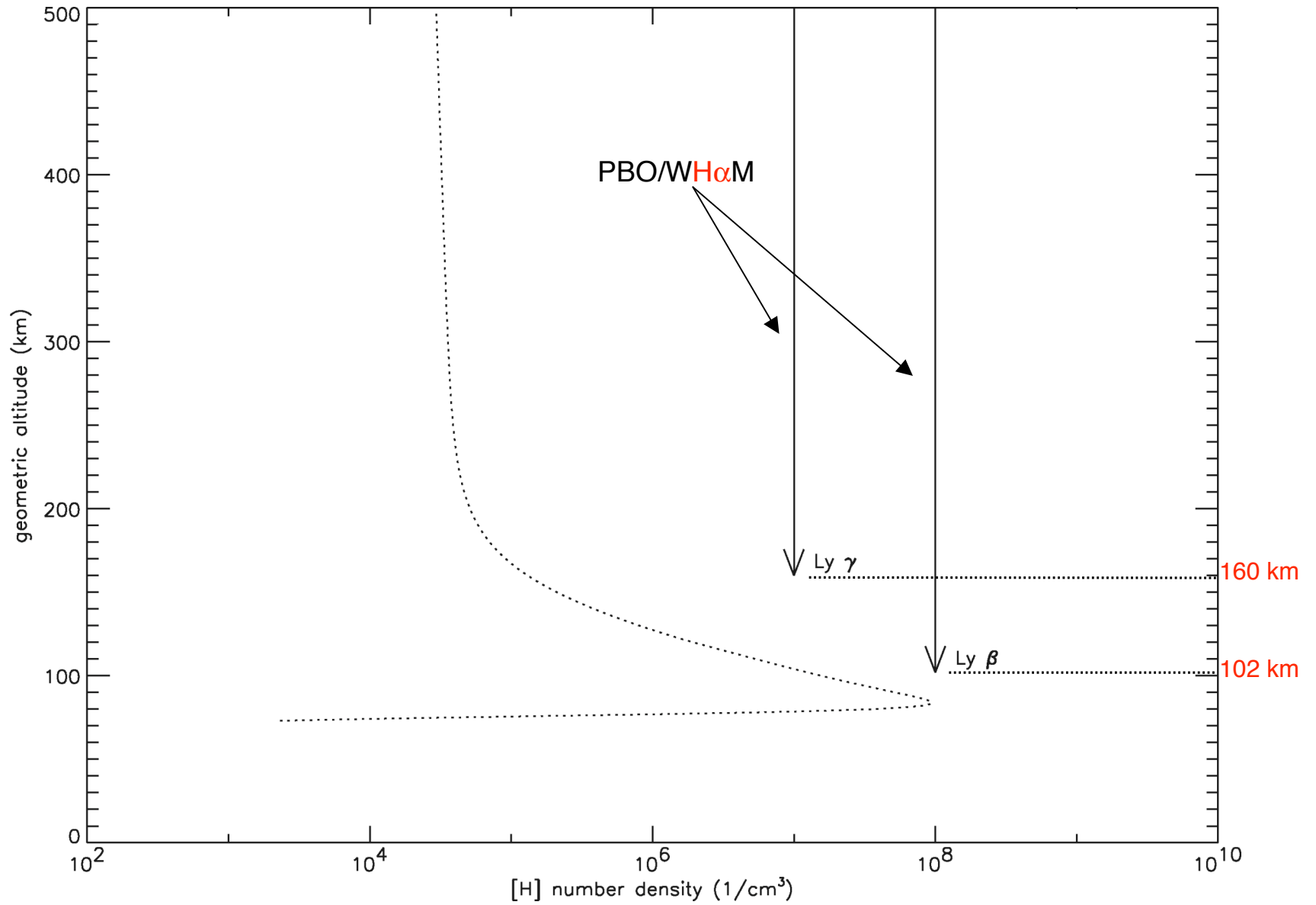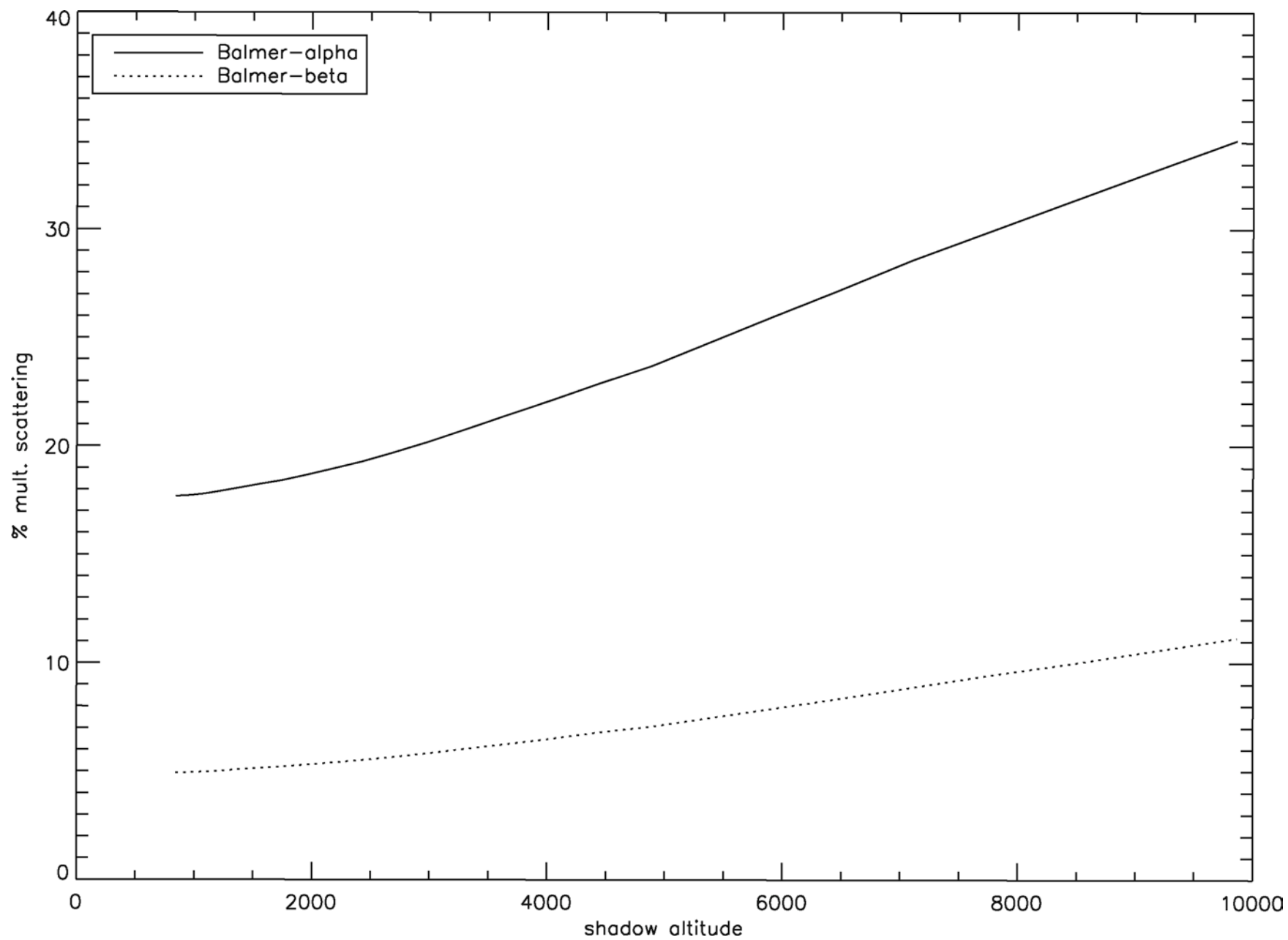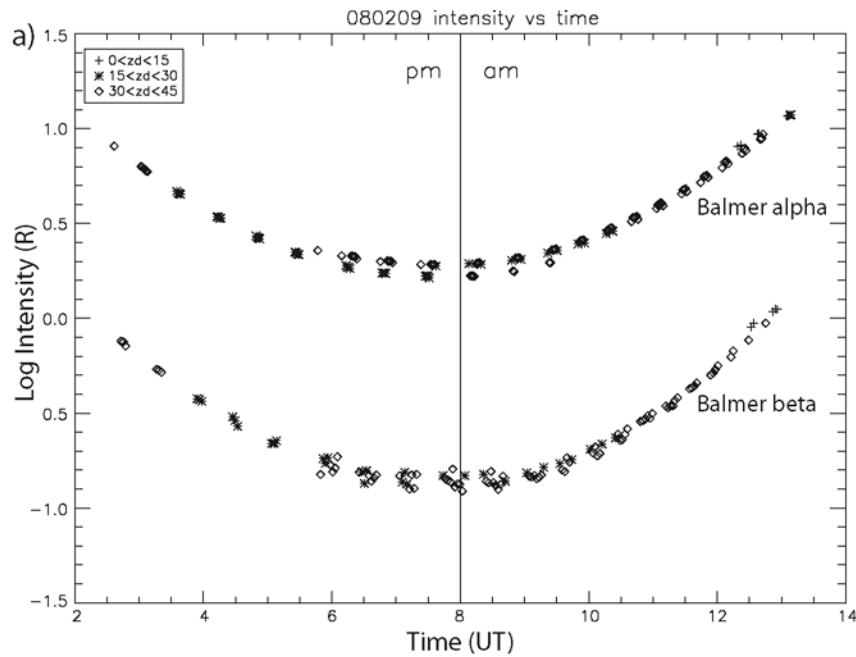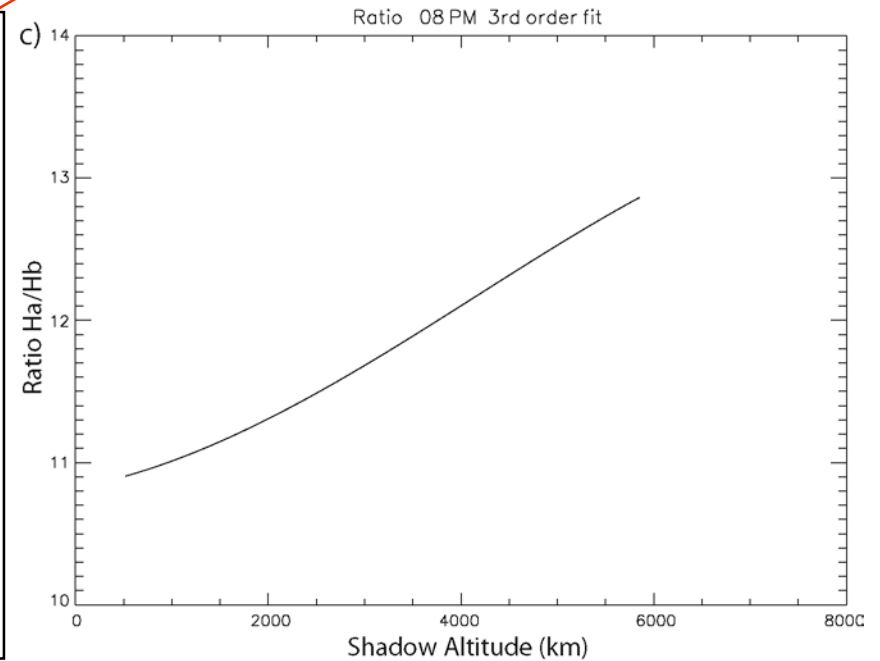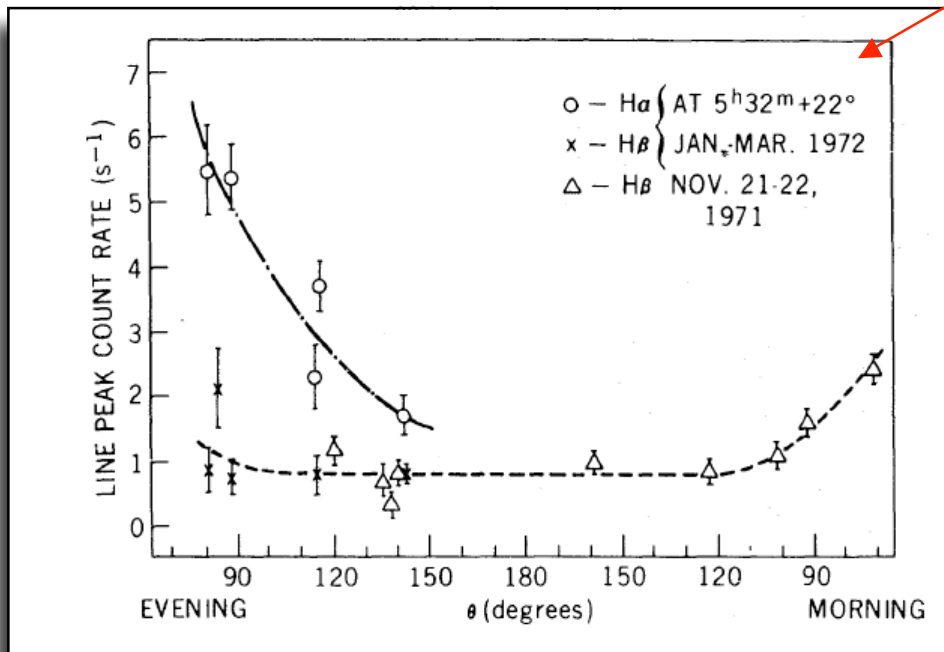# Periodic variations of geocoronal Balmer-alpha brightness due to solar-driven exospheric abundance variations

[1]R. B. Kerr, [2]R. Garcia, [3]X. He, [1]J. Noto, [4]R. S. Lancaster, [2]C. A. Tepley, [2]S. A. González, [2]J. Friedman , [5]R. A. Doe, [1]M. Lappen, [1]B. McCormack

Abstract.   Measurements of the geocoronal Balmer-alpha (H_α) brightness have been made at the Arecibo Observatory during 11 separate periods since 1983 using both a Fabry-Perot interferometer and a tilting filter photometer. The tilting filter photometer is calibrated for absolute sensitivity using a constant brightness source traceable to National Institute of Standards and Techniques (NIST) standards and is used to cross-calibrate the Fabry-Perot interferometer. Since the observational technique has not changed since 1983, and since the data analyses technique are uniform, these data provide a measure of the solar cycle variation of H_α brightness at Arecibo. Unlike earlier studies, we discern no systematic discrepancy between the H_α brightness and estimates of the solar Lyman-beta flux that pumps [...] emission. Rather, we conclude that geocoronal hydrogen abunda[...] always) larger than models suggest, although not systematically [...] measured during solar minimum conditions, when brightness is a[...] during solar maximum conditions, for measurements at solar dep[...] Above about 40° solar depression (corresponding to an illuminate[...] approximately 2000 km), no solar cycle variation is evident, and [...] persistently greater than models. Intricacies of the Lyman-beta r[...] detection of an early morning maximum of hydrogen density nea[...] brightness data alone, although the H_α brightness is generally asy[...] midnight, with brighter emission in the postmidnight sector. Stud[...] (nighttime) variation demonstrate that the H_α brightness can vary [...] days.

Derivation of neutral oxygen density under charge exchange in the midlatitude topside ionosphere

L. S. Waldrop
Department of Electrical and
Champaign, Urbana, Illinois,

E. Kudeki
Department of Electrical and
Champaign, Urbana, Illinois,

S. A. González
National Astronomy and Iono
Puerto Rico

M. P. Sulzer
National Astronomy and Iono
Puerto Rico

R. Garcia
National Astronomy and Iono
Puerto Rico

M. Butala
Department of Electrical and
Champaign, Urbana, Illinois,
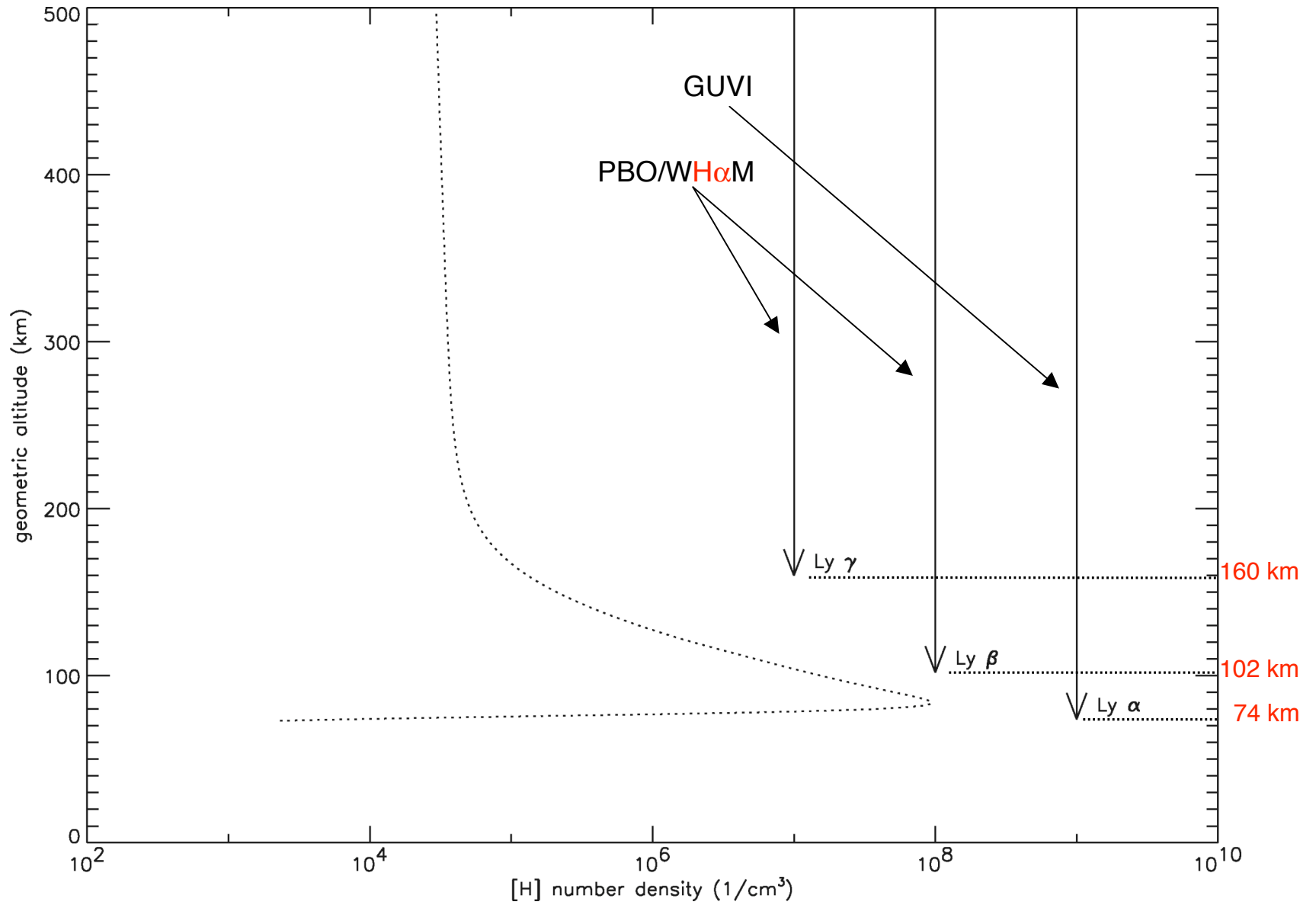
F. Kamalabadi
Department of Electrical and
Champaign, Urbana, Illinois,

We describe a new technique to derive neutral atomic oxygen density, [O], in the upper thermosphere using coincident incoherent scatter radar (ISR) and airglow emission observations from Arecibo Observatory. The technique exploits the nearly resonant charge exchange coupling between neutral and ionized hydrogen and oxygen that serves as the dominant chemical source and sink of protons near and above the F region peak. Under charge exchange production and loss of H+, the proton continuity equation can be solved for [O] using twilight H density profiles derived from measured H emission brightness at 656.3 nm together with ion density, temperature, and flux obtained simultaneously by the Arecibo ISR. We present both equilibrium and nonequilibrium solutions for [O] between 500 and 1500 km during a single quiescent nighttime interval under moderate solar activity. Comparisons with theoretical expectations and with MSIS !model calculations of O density are used to identify the altitude and local time extent over which the technique is justified. These comparisons generally support technique validity between! 600 and 800 km, where sufficient reactant densities are present to validate the charge exchange formulation of the continuity equation. Equilibrium solutions for [O] near 650–700 km exhibit excellent agreement with MSIS estimates before midnight, but deviations arising from ion transport become increasingly significant both above this height and as dawn approaches. Incorporation of measured proton flux gradients into the nonequilibrium solutions improves agreement between the derived and modeled estimates significantly after midnight, while the minor nonequilibrium contributions during several hours before midnight lend additional support for the presence of charge exchange equilibrium.
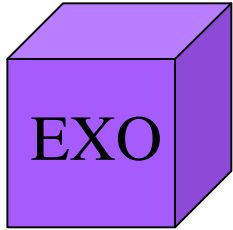
MSIS Thermospheric [H](z) Profile

geometric altitude (km)

[H] number density (1/cm³)
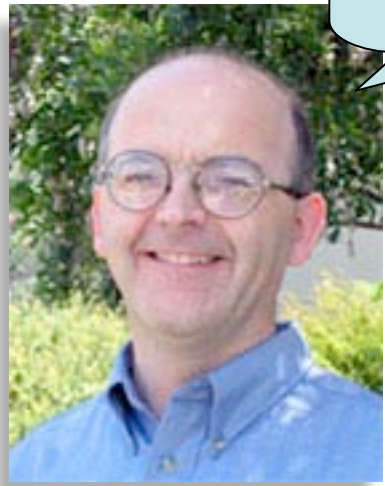
GUVI

PBO/WHαM

Ly γ — 160 km

Ly β — 102 km

Ly α — 74 km

Multi-line: Lyman α, Lyman β (Hα), Lyman γ (Hβ)

TIMED/GUVI (SABER & SEE)

EXO

TIME-GCM

PBO/WHαM CTIO

Data-model comparison search analysis of coincident
PBO Balmer α, EURD Lyman β geocoronal
measurements from March 2000

J. Bishop
E. O. Hulburt Center for Space Research, Naval Research Laboratory, Washington, D. C., USA

E. J. Mierkiewicz and F. L. Roesler
Department of Physics, University of Wisconsin-Madison, Madison, Wisconsin, USA

J. F. Gómez and C. Morales
Laboratorio de Astrofísica Espacial y Física Fundamental, INTA, Madrid, Spain

Received 28 July 2003; revised 3 February 2004; accepted 24 February 2004; published 27 May 2004.

[1] Recent Lyman series and Balmer series airglow measurements provide a fresh opportunity to investigate the density distribution and variability of atomic hydrogen in the upper atmosphere. Dedicated nightside Balmer α Fabry-Perot spectrometer measurements at the Pine Bluff Observatory (PBO), University of Wisconsin-Madison, have been acquired since late 1999 taking advantage of several technological advances. Extreme ultraviolet spectral radiance measurements by the Espectrógrafo Ultravioleta extremo para la Radiación Difusa (EURD) instrument on the Spanish MINISAT-1 satellite from October 1997 to December 2001 provide extensive sets of geocoronal Lyman β, Lyman γ and He 584 Å emission intensities. In this paper, coincident EURD Lyman β and PBO Balmer α radiance measurements from the early March 2000 new moon period are presented. In addition to serving as examples of the data sets now available, the data volume poses an analysis challenge not faced in prior geocoronal studies. A data-model comparison search procedure employing resonance radiation transport results for extensive sets of parametric density distribution models is being developed for use in analyses of multiple large data sets; this is described, and example results for the PBO and EURD March 2000 data sets are presented. The tightness of the constraints obtained for the solar line-center Lyman β irradiance and the atomic hydrogen column abundance is somewhat surprising, given the crudeness of the parameter binning in the search procedure and the fact that a small number of recognized corrections remain to be made to each data set.   INDEX TERMS: 0310 Atmospheric Composition and Structure: Airglow and aurora; 0355 Atmospheric Composition and Structure: Thermosphere—composition and chemistry; 7837 Space Plasma Physics: Neutral particles; 0394 Atmospheric Composition and Structure: Instruments and techniques; KEYWORDS: airglow measurements: Lyman series, Balmer series; airglow analysis: techniques and methods; atmospheric composition: atomic hydrogen; geocoronal density distributions and radiative transport; exospheres

Citation: Bishop, J., E. J. Mierkiewicz, F. L. Roesler, J. F. Gómez, and C. Morales (2004), Data-model comparison search analysis of coincident PBO Balmer α, EURD Lyman β geocoronal measurements from March 2000, J. Geophys. Res., 109, A05 doi:10.1029/2003JA010165.

References

- Anderson, D. E., Jr.; Meier, R. R.; Hodges, R. R., Jr.; Tinsley, B. A., Journal of Geophysical Research, Volume 92, pp.7619-7642 (1987), "Hydrogen Balmer alpha intensity distributions and line profiles from multiple scattering theory using realistic geocoronal models"

- Anderson, D. E., Jr.; Paxton, L. J.; McCoy, R. P.; Meier, R. R.; Chakrabarti, Supriya, Journal of Geophysical Research, Volume 92, pp.8759-8766 (1987), "Atomic hydrogen and solar Lyman alpha flux deduced from STP 78-1 UV observations"

- Brinton, H. C.; Mayr, H. G.; Potter, W. E., Geophysical Research Letters, Volume 2, pp.389-392 (1975), "Winter bulge and diurnal variations in hydrogen inferred from AE-C composition measurements"

- Bush, B. C.; Chakrabarti, S., Journal of Geophysical Research, Volume 100, Issue A10, pp.19609-19626 (1995), "Analysis of Lyman alpha and He I 584-Å airglow measurements using a spherical radiative transfer model"

- Bishop, J., Journal of Atmospheric and Solar-Terrestrial Physics, Volume 63, Issue 4, pp.331-340 (2001), "Thermospheric atomic hydrogen densities and fluxes from dayside Lyman /alpha measurements"

- Bishop, J., Journal of Quantitative Spectroscopy and Radiative Transfer, Volume 61, issue 4, pp.473-491 (1999), "Transport of resonant atomic hydrogen emissions in the thermosphere and geocorona: model description and applications"

- Bishop, J., Planetary and Space Science, Volume 39, June 1991, pp.885-893 (1991), "Analytic exosphere models for geocoronal applications"

- Bishop, J., Journal of Geophysical Research, Volume 90, pp.5235-5245 (1985), "Geocoronal structure - The effects of solar radiation pressure and the plasmasphere interaction"

- Bishop, J.; Chamberlain, J. W., Icarus, Volume 81, pp.145-163 (1989), "Radiation pressure dynamics in planetary exospheres - A 'natural' framework"

- Bishop, J.; Chamberlain, J. W., Journal of Geophysical Research, Volume 92, pp.12377-12397 (1987), "Geocoronal structure. 2 - Inclusion of a magnetic dipolar plasmasphere"

References

- Bishop, J.; Chamberlain, J. W., Journal of Geophysical Research, Volume 92, Issue A11, pp.12389-12397 (1987), "Geocoronal structure. 3. Optically thin, Doppler-broadened line profiles"

- Bishop, J.; Harlander, J.; Nossal, S.; Roesler, F. L., Journal of Atmospheric and Solar-Terrestrial Physics, Volume 63, Issue 4, pp.341-353 (2001), "Analysis of Balmer /alpha intensity measurements near solar minimum"

- Bishop, J.; Mierkiewicz, E. J.; Roesler, F. L.; Gómez, J. F.; Morales, C., Journal of Geophysical Research, Volume 109, Issue A5, p.A05307 (2004), "Data-model comparison search analysis of coincident PBO Balmer alpha, EURD Lyman beta geocoronal measurements from March 2000"

- Carruthers, G. R.; Page, T.; Meier, R. R., Journal of Geophysical Research, vol. 81, pp.1664-1672, (1976), "Apollo 16 Lyman alpha imagery of the hydrogen geocorona"

- Chamberlain, J. W., Planetary and Space Science, Volume 11, p.901 (1963), "Planetary coronae and atmospheric evaporation"

- Chamberlain, J. W.; Bishop, J., Icarus, Volume 106, p.419 (1993), "Radiation pressure dynamics in planetary exospheres. II - Closed solutions for the evolution of orbital elements"

- Cole, K.D., Nature 211, p 1385-1387 (1966), "Theory of some Quiet Magnetospheric Phenomena related to the Geomagnetic Tail"

- Haffner, L. M.; Reynolds, R. J.; Tufte, S. L.; Madsen, G. J.; Jaehnig, K. P.; Percival, J. W., The Astrophysical Journal Supplement Series, Volume 149, Issue 2, pp. 405-422 (2003), "The Wisconsin Halpha Mapper Northern Sky Survey"

- He, Xiangqun, Thesis (PH.D.), Boston University (1995), "Hydrogen Escape from the Earth's Atmosphere"

- He, Xiangqun; Kerr, Robert B.; Bishop, James; Tepley, Craig A., Journal of Geophysical Research, Volume 98, no. A12, pp.21,611-21,626 (1993), "Determining exospheric hydrogen density by reconciliation of H-alpha measurements with radiative transfer theory"

References

- Hunten, D. M., Icarus (ISSN 0019-1035), vol. 85, pp. 1-20. (1990), "Kuiper Prize Lecture - Escape of atmospheres, ancient and modern"

- Hunten, D. M., Journal of Atmospheric Sciences, vol. 30, Issue 8, pp.1481-1494 (1973), "The Escape of Light Gases from Planetary Atmospheres"

- Hunten, D. M., J. Atmos. Sci., Vol. 30, pp. 726 – 732 (1973), "The escape of H2 from Titan"

- Kerr, R. B.; Garcia, R.; He, X.; Noto, J.; Lancaster, R. S.; Tepley, C. A.; González, S. A.; Friedman, J.; Doe, R. A.; Lappen, M.; McCormack, B., Journal of Geophysical Research, Volume 106, Issue A12, pp. 28797-28818 (2001), "Periodic variations of geocoronal Balmer-alpha brightness due to solar-driven exospheric abundance variations"

- Kupperian, J. E., Jr.; Byram, E. T.; Chubb, T. A.; Friedman, H., Planetary and Space Science, Volume 1, p.3 (1959), "Far ultra-violet radiation in the night sky"

- Meier, R. R.; Mange, P., Planetary and Space Science, Volume 18, p.803 (1970), "Geocoronal hydrogen: an analysis of the Lyman-alpha airglow observed from OGO-4"

- Meriwether, J. W., Jr.; Atreya, S. K.; Donahue, T. M.; Burnside, R. G., Geophysical Research Letters, Volume 7, pp. 967-970 (1980), "Measurements of the spectral profile of Balmer Alpha emission from the hydrogen geocorona"

- Mierkiewicz, E. J.; Roesler, F. L.; Nossal, S. M.; Reynolds, R. J., Journal of Atmospheric and Solar-Terrestrial Physics, Volume 68, Issue 13, pp.1520-1552 (2006), "Geocoronal hydrogen studies using Fabry Perot interferometers, part 1: Instrumentation, observations, and analysis"

- Nossal, S. M.; Mierkiewicz, E. J.; Roesler, F. L.; Reynolds, R. J.; Haffner, L. M., Journal of Atmospheric and Solar-Terrestrial Physics, Volume 68, Issue 13, p. 1553-1575 (2006), "Geocoronal hydrogen studies using Fabry Perot interferometers, part 2: Long-term observations"

References

- Nossal, S.; Roesler, F. L.; Bishop, J.; Reynolds, R. J.; Haffner, M.; Tufte, S.; Percival, J.; Mierkiewicz, E. J., Journal of Geophysical Research, Volume 106, Issue A4, pp.5605-5616 (2001), "Geocoronal Halpha intensity measurements using the Wisconsin Halpha Mapper Fabry-Perot facility"

- Reynolds, R. J.; Scherb, F.; Roesler, F. L., Astrophysical Journal, Volume 181, p.L79 (1973), "A Search for Halpha Emission from Interstellar Clouds"

- Reynolds, R. J.; Scherb, F.; Roesler, F. L., Astrophysical Journal, Volume 185, pp. 869-876 (1973), "Observations of Diffuse Galactic HA and [n II] Emission"

- Reynolds, R. J.; Roesler, F. L.; Scherb, F., Astrophysical Journal, Vol. 179, pp. 651-658 (1973), "Low-Intensity Balmer Emissions from the Interstellar Medium and Geocorona"

- Roble, R. G.; Dickinson, R. E., Geophysical Research Letters, Volume 16, pp.1441-1444, (1989), "How will changes in carbon dioxide and methane modify the mean structure of the mesosphere and thermosphere?"

- Salby, M. L., Academic Press; 1 edition (May 13 1996), "Fundamentals of Atmospheric Physics"

- Sheglov, P. V., Nature, Volume 199, Issue 4897, p. 990 (1963), "Concentration of Nightglow Halpha-emission to the Ecliptic and the Radial Velocities of this Line"

- Strobel, D. F., Radio Science, Volume 7, p.1 (1972), "Minor neutral constituents in the mesosphere and lower thermosphere"

- Tinsley, B. A., Fundamentals of Cosmic Physics, vol. 1, no. 3, pp. 201-300 (1974), "Hydrogen in the upper atmosphere"

- Tinsley, B. A., Planetary and Space Science, Volume 21, Issue 4, pp.686-691 (1973), "The diurnal variation of atomic hydrogen"

- Waldrop, L. S.; Kudeki, E.; González, S. A.; Sulzer, M. P.; Garcia, R.; Butala, M.; Kamalabadi, F., Journal of Geophysical Research, Volume 111, Issue A11, CiteID A11308 (2006), "Derivation of neutral oxygen density under charge exchange in the midlatitude topside ionosphere"

The End